AD-782 518

THE RESPONSE OF CLAMPED CIRCULAR
PLATES TO CONFINED EXPLOSIVE LOADINGS

Steve Zilliacus, et al

Naval Ship Research and Development Center
Bethesda, Maryland

February 1974

AD 782518

NAVAL SHIP RESEARCH AND DEVELOPMENT CENTER

Bethesda, Md. 20034

THE RESPONSE OF CLAMPED CIRCULAR PLATES

TO CONFINED EXPLOSIVE LOADINGS

by

S. Zilliacus
W.E. Phyillaier
P.K. Shorrow

STRUCTURES DEPARTMENT
RESEARCH AND DEVELOPMENT REPORT

20050404113

February 1974

Report 3987

MAJOR NSRDC ORGANIZATIONAL COMPONENTS

*REPORT ORIGINATOR

```
                            NSRDC
                         COMMANDER      00
                      TECHNICAL DIRECTOR 01
```

| OFFICER-IN-CHARGE CARDEROCK 05 | | OFFICER-IN-CHARGE ANNAPOLIS 04 |

| SYSTEMS DEVELOPMENT DEPARTMENT 11 | |

| SHIP PERFORMANCE DEPARTMENT 15 | AVIATION AND SURFACE EFFECTS DEPARTMENT 16 |

| * STRUCTURES DEPARTMENT 17 | COMPUTATION AND MATHEMATICS DEPARTMENT 18 |

| SHIP ACOUSTICS DEPARTMENT 19 | PROPULSION AND AUXILIARY SYSTEMS DEPARTMENT 27 |

| MATERIALS DEPARTMENT 28 | CENTRAL INSTRUMENTATION DEPARTMENT 29 |

DEPARTMENT OF THE NAVY

NAVAL SHIP RESEARCH AND DEVELOPMENT CENTER

BETHESDA, MARYLAND 20034

THE RESPONSE OF CLAMPED CIRCULAR PLATES

TO CONFINED EXPLOSIVE LOADINGS

by

S. Zilliacus
W.E. Phyillaier
P.K. Shorrow

February 1974

Report 3987

TABLE OF CONTENTS

LIST OF FIGURES

LIST OF TABLES

ABSTRACT

A series of confined explosive tests was carried out for 12-in.-diameter steel and aluminum plates. Each plate in turn formed one end of the closed cylindrical chamber inside which the explosives were detonated. Tests were conducted with the chamber suspended in air and in water to determine pressure histories, deformation shapes, and failure modes in the inelastic range of air- and water-backed plates as well as to determine pressure decay rates resulting from venting to the atmosphere.

The final deformation shapes observed were uniform and repeatable, but the pressure records were less uniform. There was a distinct difference between the final shapes of the air- and water-backed plates; those of the former were intermediate between conical and parabolic whereas those of the latter were more parabolic and sometimes dimpled in the center. Failures occurred at the plate edge for charge standoffs greater than one plate diameter and at the plate center for closer standoffs. Measured pressure decays due to venting confirmed an analytical method established for predicting gas venting.

ADMINISTRATIVE INFORMATION

INTRODUCTION

The explosion of a weapon inside a ship compartment can cause extensive damage both there and in adjacent compartments by rupturing bulkheads and decks. If the explosion ruptures the hull, extensive flooding of the ship can follow. The objective of this investigation was to develop an understanding of the damage mechanism associated with confined explosions and thus make possible more accurate predictions of ship damage.

Qualitatively, the explosion-response phenomena for a compartment should resemble those of a suddenly inflated rectangular balloon; with the edges offering maximum resistance to deformation and the sides undergoing membrane deformation. The complexity involved in a quantitative description of these phenomena emphasizes the desirability of devising a simple physical model to gain insight into the problems involved. Such a model might possess an

axis of symmetry and contain only one deformable surface instead of six as in a compartment. These considerations prompted the selection of a model consisting of a circular plate attached to one end of a closed cylindrical explosion chamber.

METHOD

EXPLOSION CHAMBER

A cylindrical explosion chamber, designed by the authors and fabricated in the NSRDC shops, was used to conduct a series of contained explosive tests against 12-in.-diameter circular plates of medium steel and aluminum in various thicknesses. The chamber is pictured in Figure 1, and the method of clamping a specimen plate to one end of the explosion chamber is illustrated in Figure 2.

The chamber was armed by mounting the explosive charge onto a pipe plug and threading the pipe plug into its position in the back wall of the chamber; see Figure 3.

TEST PROCEDURE

Tests were conducted against specimen plates which were either air backed or water backed. Air-backed plate tests were conducted with the explosion chamber suspended in the NSRDC test pit. Water-backed plate tests were conducted with the explosion chamber suspended in the NSRDC test pond as shown in Figure 4.

The blast loading was produced by cylindrical charges of Pentolite in weights selected to cause large plastic deformation or failure of the plates. The pressures generated in the explosion chamber by these charges were recorded for many of the tests by a single gage at one of four locations at the end of the chamber opposite to the pipe plug. Pressures were measured during explosive loading of both deformable test plates and a thick rigid plate to determine pressure distribution across the rigid plate and the effect of coupling on the measured pressure. A description of the pressure gage calibration and of the recording system is given in Appendix A, and the gage locations are detailed in Figure 5. Note that a recessed mounting was employed in an attempt to protect the gages from possible impact.

Several tests were also performed in which the side of the test plate facing the charge was covered by a 1/2-in.-thick slab of high-density styrofoam. These were included to determine the effect on pressure measurements of the pressure that was reflected back off the test plate.

2

All plates that had not ruptured were measured after testing to determine their deformation shape. Some plates were marked by a grid so that residual strains and thicknesses could be measured. High-elongation strain gages were mounted and strain records were obtained for a few air-backed plates.

After the series of tests had been completed, the explosion chamber was cut to one-half its original length. Tests were then repeated to determine the effect of a change in chamber volume on plate response.

Several venting tests were also conducted at both chamber volumes. A heavy steel plate with a venting hole at its center was mounted on the chamber, and pressure records were taken for various charge sizes and venting areas.

All tests and the material properties of the test plates are listed in Tables B.1 and B.2 of Appendix B.

RESULTS AND DISCUSSION

Table 1 indicates the peak pressures recorded during testing. Some typical pressure records and impulse curves derived from the pressure records are shown in Figures 6–11.

The response of the plates to the explosive loading is given in Figure 12 and in Table 2 which includes the maximum permanent center deflection for all plates according to plate type. The profiles of all permanently deformed plates are included (Figure 12) together with photographs of some deformed and some failed plates (Figure 13). Failure was always at the edge (Figure 13f) unless the charge was at a standoff of less than one plate diameter, in which case center failure resulted (Figure 13d). Final thickness and strain curves for a typical deformed plate are given in Figure 14. Several determinations of plate strain-time histories obtained by using high-elongation strain gages are shown in the records of Figure 15. Results of attempts to find general scaling laws describing the magnitude of the plate response are indicated by the curves of Figure 16. Figure 17 and Table 3 summarize the results of the gas venting tests.

These tables and figures are now presented together with a discussion of their contents.

PLATE LOADINGS

Pressure records were taken for air-backed tests only. Because of the large number of pressure records taken, only those pertinent to the discussion will be shown in this report.

However, most records had the same general features, namely, an early high peak pressure which very rapidly decayed to a series of much lower oscillations. The peak pressures for all records taken during testing (except the venting test pressures given elsewhere) are listed in Table 1.

The cavity phenomena resulting from the recessed mounting (Figure 5) of pressure gages together with finite gage size and finite recording system frequency response distorted the pressure histories. Actual initial pressure rise times were probably much too small to be recorded accurately (Appendix A includes a discussion of recording system characteristics for high frequency signal components). The lack of repeatability for peak pressures (Table 1) may be due not only to recording system deficiencies but also to nonuniformity among different charges that were nominally identical. Small differences in detonation rates, for instance, could significantly affect peak pressures.

Figure 6 shows the records of repeated tests of 7-g cylindrical Pentolite charges detonated at a standoff distance (SOD) of 35 in. while the explosion chamber was closed by the rigid heavy steel plate. The shapes of these records were similar but the peak pressure differed by as much as a factor of two. Test 26 was recorded when a deformable plate closed the explosive chamber. Although the peak pressure recorded in this particular test was higher than those attained with a "rigid" plate (Tests 16, 17, and 40), its shape was similar. Other tests, especially for larger charge sizes, showed about the same peak pressures and record shapes for both deforming and "rigid" plates. Thus the presence of a deforming plate did not alter the early pressure history of the chamber in any regular way. As might be expected, larger charge sizes produced pressure records which, on the average, had larger peak pressures. The transient pressures which followed were also somewhat higher.

In the case of test plates protected by styrofoam on the side facing the charge, it had been hypothesized that as a result of being crushed, the styrofoam would attenuate a reflected shock wave and thus alter the pressure record. Actually, however, the results for such plates did not differ in any regular way from corresponding tests without styrofoam. Test 47 in Figure 7 is an example of a pressure record taken with styrofoam on the plate.

Figure 7 also shows several pressure records taken with the gage located at the center of the rigid plate in a face-on position (see also Table 1a). These and similar records taken from the other face-on positions in the rigid plate for 7-, 25-, and 50-g Pentolite charges did not appear to be very different from records of corresponding tests where the gage was mounted in the flange. Thus, the pressure history appeared to be fairly uniform across the end of the chamber. (Impulse curves derived from these pressure records, however, showed that the 7-g records did differ somewhat according to gage location. This will be discussed further later in the report.)

For most of the plate response tests, the charge was detonated while very close to the "back wall" of the chamber (at a 35-in. SOD) as shown in Figure 3. A few tests were performed at shorter SOD's, see Figure 8 for the pressure records obtained for three of these tests. It is clear from Table 1b that on the average, the peak pressures measured at the middle ranges were much lower than those measured at the full 35-in. SOD despite the shorter distance. At a close-in (6-in.) SOD, the peak pressures recorded were again higher, about the same as those at the full 35-in. SOD. These results appear reasonable if one considers the reflecting effect of the back wall. When the charge is detonated at full range, the shock wave is reflected off the back wall almost immediately; it then follows very closely behind the direct shock wave that is moving toward the specimen plate. Since this reflected wave is traveling in the higher pressure wake of the direct wave, it moves faster, thus catching up with and becoming superimposed on the direct wave. This phenomenon would cause higher peak pressures than would the direct wave alone. As standoff distance from the back wall is increased, this "catch-up" effect no longer dominates, resulting in a lower initial peak pressure (direct wave only). Thus it makes sense for a peak pressure to be lower even though the charge is nearer, as was observed in the tests. And, of course, as the charge is brought still closer to the gage, the direct pressure wave will be stronger at the close range, and again give high values.

The total impulse delivered to the test plate in the first few milliseconds is of interest for the analysis. Most of the pressure-time histories were integrated to obtain curves of the total impulse delivered at the gage as a function of time. Figure 9 is an example of a pressure-time history and its corresponding impulse curve.

Impulse curves for many of the pressure records are given in Figure 10. Impulse curves for the small 7-g charge tests showed patterns that were not apparent in the pressure records. Impulse curves obtained from pressure records taken while the gage was mounted face on to the charge (in the "rigid" plate) were usually lower than those derived from measurements taken at the flange position. The two face-on curves (broken lines in Figure 10a) diverged from the other curves as time increased. Other curves not shown there followed the same pattern. The curve for Test 16 was the only exception in a total of 11 curves. Thus, it appears that the gage location is important and that the impulse delivered to the center of the test plates is somewhat less than that delivered to the flange area. This pattern, however, was not as clear for larger charge tests (see Figures 10c and 10d). Only a few face-on curves are available for larger charges, and it is not yet clear whether the pattern would have reemerged had more records been taken with larger charges.

A coupling effect was a second trend noted for the 7-g charges. The presence of a rapidly deforming plate gave impulse curves which rose very steeply at first and then leveled off (see the curve for Test 26 in Figure 10a; the curve for Test 53, not shown, was very similar). Apparently the pressure record was altered in its very early phase by the plate

response. Again, the pattern was not apparent for larger charges. It appears likely that coupling effect and gage orientation are less significant at higher overpressures.

In order to compare the general features of the impulse curves for charges of different weights, those corresponding to the full SOD (the pressure gage recording from the flange position) were averaged for each charge size. As indicated in Figure 11, the results were quite similar up to about 0.1 msec.

PLATE RESPONSE

Experimental Data

The maximum permanent deflections of all plates tested are listed in Table 2 and the final deformed shapes are shown in Figure 12. Except for dimpled plates (which will be mentioned later), the maximum plate deflection was always at or near the center of the plate and the deformation shape was always nearly symmetrical about that center. The plots of Figure 12 show the average deflection (based on measurements along two mutually perpendicular diameters) from the original plane of the plate. Plate deformations were reasonably repeatable and uniform.

There was very little evidence of edge movement or "pull in"; most tests showed no detectable edge movement at all. Photographs of typical deformed or failed plates are presented in Figure 13.

The deformation shapes observed led to several generalizations:

1. When the charge was detonated near the back wall of the longer chamber, air-backed plates tended to deform to a conical shape, particularly for large deformations. Corresponding water-backed plates had a more parabolic shape. Moreover, some water-backed plates formed a pronounced dimple (see Figures 12f and 13e). This dimpling effect is the result of water cavitation collapse or other hydrodynamic reactions and so was not observed in the air-back tests.

2. When the charge was detonated near the center of the longer chamber or in the shortened chamber, the shape of air-backed plates was more parabolic than when the charge was detonated at the far end of the long chamber. Probably this is because the shock loading across the face of the test plate is less uniform when the charge is near to the test plate than when farther away. Most likely there is a fully developed plane shock front at maximum SOD.

3. The maximum center displacement of air-backed plates was approximately 2 1/2 times that of corresponding water-backed plates.

6

4. For tests conducted with the charge at the far end of the chamber, air-backed plates had about the same maximum center displacements, in both the long and short chambers. Plates tested on the short chamber failed at lower center displacements, however, and, as already noted, unfailed plates had a more parabolic shape.

5. Plate deformation was greater when the charge was detonated near the back wall of the chamber than at its center. This corresponds to the fact that peak recorded pressures were greater when the charge was at the back than at the center.

6. In all tests, plate failure always occurred at the edge of the plate except when the charge was less than two plate radii from the target plate. Failed plates showed evidence of "necking down" at the edge before failure and then shearing away in one piece, leaving a sharp, thin edge around the circumference (see Figure 13f). Unfailed plates with large deformations also exhibited considerable "necking down" at the circumference. If plate failure was caused by a near charge (one plate radius or less), failure was by rupture at the plate center and large petals tore away from the center (see Figure 13d); however, a large amount of necking down can also occur at the circumference. One air-backed plate failed at both the edge and center when the charge was at 1 1/2 plate radii.

In addition to data on permanent deformation shapes of all unfailed plates, the results include measurements of final thickness and principal strains across a few typical deformed plates. Representative values from a nearly failed plate are shown in Figure 14. It can be seen that strains were greatest in the meridianal direction and near the center. As might be expected, the plate center was also the thinnest part of the plate (if the necking down at the edge is ignored).

Several successful attempts were made to obtain strain histories of test plates. Special adhesives and high-elongation strain gages enabled good records for steel test plates which were deformed only moderately. As indicated in Figure 15, most of the strain occurred within the first 1/2 msec after the arrival of the shock wave. Attempts to obtain strain histories for plates deformed nearly to failure were unsuccessful because the gages or the lead wires, especially those at the plate center, came off during the explosion.

Analytical Determination

The experimental data were utilized to develop a tentative empirical law governing the maximum deflection that an unfailed plate would assume. The normalized deflection d/a, which is the ratio of maximum plate deflection to plate radius, was plotted as a function of different combinations of parameters for all test plates that did not fail. Two empirical laws resulted, one for air-backed and one for water-backed plates;

7

Air-backed plates:

$$\frac{d}{a} = 0.156 \left[\frac{W_c}{W_p} \cdot \frac{a}{h} \cdot \frac{\sigma_R}{\sigma_p} \right]^{0.641}$$

Water-backed plates:

$$\frac{d}{a} = 0.0729 \left[\frac{W_c}{W_p} \cdot \frac{a}{h} \cdot \frac{\sigma_R}{\sigma_p} \right]^{0.506}$$

In both instances, d is the maximum deflection, a is the radius, W_c is the charge weight, W_p is the plate weight, h is the plate thickness, σ_p is the average of 0.2 percent offset and ultimate stress of test plate (in pounds per square inch), and σ_R is a reference stress taken as 40,000 psi.

The curves for these two equations are shown in Figure 16a along with all data points from the tests. These equations were determined from tests for which the charge was detonated at the back wall of the long chamber. Similar curves for unfailed plates tested on the short chamber are given in Figure 16b.

Chamber length and charge location were held constant in determining the empirical laws. Actually, however, when the chamber length was halved, the effect on the center deflection was quite slight as can be seen in Figure 16b; data for air-backed plates that deformed on the shortened chamber fall fairly well along the curve determined from the long chamber data. A change in charge location, however, had a very strong effect on the center deflection. Data are available for only a few air-backed plates for cases where the charge was not at the back wall, but the deformation for these cases was substantially less than predicted by the empirical law. However, it is worth noting that the few available points did fall on a line roughly parallel to that shown for air-backed plates in Figure 16a.

The method of Sewell and Kinney[1] was applied in the first attempt at establishing a criterion to predict the onset of failure. A critical impulse to be delivered in a critical time was established for each of the NSRDC test plates. The calculated critical impulses were then compared with the measured impulses delivered to the test plates in the critical time to see

---

[1]Sewell, R.G.S. and G.F. Kinney, "Response of Structures to Blast: A New Criterion," Annals of the New York Academy of Sciences, Vol. 152, Art. 1 (Oct 1968).

how well failure was predicted. As can be seen in the tables of Appendix C, however, all plate types survived impulses much greater than those predicted. Further, the ratio of delivered impulse to critical impulse at which failure did begin to occur was not the same for different plate types and standoff distances. The general concept of a critical impulse in a critical time is attractive because of its simplicity. However, the critical impulse apparently depends on other parameters in addition to those material properties used by Sewell and Kinney. A more thorough analysis seems necessary for developing an accurate criterion for failure.

VENTING TO THE ATMOSPHERE

A detonation inside a ship compartment is followed by venting of the explosion products through openings into adjacent compartments and perhaps into the atmosphere. The pressure loading, the subsequent response, and possibly the manner of failure of structural elements will be sensitive to the rate of venting.

Proctor[2] has derived an equation for determining the rate of pressure decay during venting to the atmosphere. His analysis assumes an isentropic nozzle flow process, and his results are in good agreement with pressure decays measured during venting tests of an explosion testing facility at the Naval Ordnance Laboratory. But the charge weight/chamber volume ratios of those tests were small.

To check the Proctor analysis at higher pressures, Pentolite charges were detonated in the center of the NSRDC explosion chamber described in this report. Venting was permitted through a hole in a heavy steel plate clamped on the end of the chamber, and the pressure history was recorded in the same manner as for the plate response tests. Seven venting tests were performed in the long chamber for various charge weights and hole areas, and a single test was performed in the shortened chamber.

Figure 17 shows a few typical pressure records taken during the tests. Superimposed over each record is the pressure history predicted by the Proctor analysis. The initial overpressure P_0 used in the predicted pressure history is derived from the Weibull empirical relationship[3] for TNT explosions in partially confined spaces.

---

[2]Proctor, J.F., "Structural Analysis of NOL Explosion Testing Facilities," Naval Ordnance Laboratory, NOLTR 69-84 (Apr 1969).

[3]Weibull, H.R.W., "Pressures Recorded in Partially Closed Chambers at Explosion of TNT Charges," Annals of the New York Academy of Sciences, Vol. 152, Art. 1 (Oct 1968).

Converted for Pentolite, the Weibull equation is:

$$P_0 = 2410 \left(\frac{0.773\ W}{V} \right)^{0.72}$$

where P_0 is the overpressure in pounds per square inch,

   W   is the weight of Pentolite in pounds, and

   V   is the volume of the chamber in cubic feet.

The charge weight was adjusted in the above equation by multiplying by 0.773, the ratio of the heat of combustion of Pentolite and TNT. To a first approximation, the Proctor analysis predicted the pressure histories reasonably well for peak overpressures as high as 230 psi, as can be seen in Figure 17.

Table 3 is another comparison of predicted and observed pressure decay. In the Proctor analysis, venting through the nozzle is sonic until the initial peak pressure decays to a critical pressure. The nozzle flow then becomes subsonic and venting continues at a decreased rate until the pressure has decayed to the ambient pressure level. If the ambient pressure is atmospheric, or 14.7 psi, the critical pressure is about 27.8 psia. Table 3 shows the calculated and measured times to reach this critical pressure for all the venting tests performed. In all cases the agreement was reasonably good.

In summary, the Proctor analysis of gas venting to the atmosphere appears useful for predicting venting at the higher pressures of interest in ship damage studies. Proctor has prepared a newer (and soon to be published) version of the analysis which promises to give a still better description of both the maximum pressure and the pressure decay. It remains to be seen whether the Proctor analysis can be successfully applied to venting through very large openings and whether it can be used in modified form to describe venting into adjacent chambers. Additional tests are needed to answer these two questions.

EXISTING METHODS FOR PREDICTING EXPLOSION CHAMBER IMPULSE AND PRESSURE

The pressure field resulting from the confined explosion is exceedingly complex because of multiple reflections from chamber surfaces. The authors have found no truly satisfactory method for predicting pressure histories strictly from charge weight and geometry. A comprehensive collection of explosion data[4] did not contain information directly applicable to

---

[4]"Structures to Resist the Effects of Accidental Explosions," Naval Facilities Engineering Command Report P-397 (Jun 1969).

impulse or pressure calculations for the tests reported herein. However, impulse values for NSRDC cylindrical chamber geometry were approximated from data available on rectangular compartments[4] by "rectangularizing" the explosion chamber (i.e., determining the impulse values for a square shock tube of the same length and volume as the explosion chamber but made of four equal flat sides). The NAVFAC impulse charts[4] included the effects of "adjacent" surface reflections but not those due to the back wall behind the charge with respect to the surface at which impulse is sought. This led to difficulties for cases in which the charge was located near the back wall. In such cases, the impulse at the back wall was crudely assumed to translate intact to the opposite end of the chamber and become superimposed on the impulse delivered by the direct wave at that end. For tests in which the charge was not near the back wall, it can be shown that the reflected impulse off the back wall does not arrive at the opposite end of the chamber within a millisecond or so of the arrival of the direct impulse and thus that the back wall does not have to be taken into account in determining the initial impulse. Impulse values so calculated are compared in Table 4 along with measured values (integrated pressure histories).

The best description of pressure found by the authors was that by Weibull,[3] but his empirical formula gives only the maximum value of the mean pressure. Actually, because of the presence of high initial peaks in any pressure record, this value represents only a small fraction of the true peak pressure (Figure 18).

The long-term decay characteristics were sought by using the pressure history obtained from Proctor.[2] In these calculations, the maximum pressure was assumed to be that of Weibull[3]

$$P_w = P_m(0)$$

(see Figure 18). The vent area of the chamber during specimen plate tests was that of the small 3/16-in. opening in the chamber used for inserting the detonator (Figure 3). The resulting decrease in pressure was found to be entirely negligible over the plate response time ($\sim$ 1 msec). It was therefore assumed that "long-term" decay could be neglected, i.e., that the "long-term" pressure could be considered constant.

A tentative approach to synthesizing pressure histories was formulated as follows:
1. The initial spiked "impulsive part" of the pressure record was assumed to be:

$$P = P_m$$

where P_m is the measured peak pressure.
2. The pressure at time t_1 (and thereafter) was assumed to be that of Weibull:[3]

$$P_w = 2410 \left(\frac{0.773 \ W}{V} \right)^{0.72}$$

11

where W is the weight of the Pentolite charge in pounds,

V is the volume of the chamber in cubic feet, and

P_w is the overpressure in pounds per square inch.

3. The pressure at $t = t_1$ was assumed to be continuous, giving

$$P_m e^{-a t_1} = P_w$$

4. The impulse i at $t = t_i$ was assumed to be:[4]

$$i = i(t_1)$$

From the above,

$$i = \frac{P_m}{a} (1 - e^{-a t_1}) = \frac{P_m}{a} \left(1 - \frac{P_w}{P_m}\right) = \frac{P_m - P_w}{a}$$

$$a = \frac{P_m - P_w}{i}$$

$$t_1 = -\frac{\ln \dfrac{P_w}{P_m}}{a} = -\frac{i \ln \dfrac{P_w}{P_m}}{P_m - P_w}$$

The pressure histories so synthesized have been superimposed on measured histories in Figure 19.

SUMMARY AND CONCLUSIONS

The loading and response phenomena of circular plates under confined explosive pressure loading were investigated experimentally and analytically. The results were as follows:

1. Pressure loading is characterized by a steep, high-amplitude pulse followed by a slowly decaying oscillatory signal of much lower amplitude.

2. An approximate loading history can be predicted from charge weight chamber geometry, and one experimental parameter (maximum pressure).

3. Reflection from a surface near the charge significantly increases the impulse delivered to the opposite surface. Thus reflection from a chamber surface may have a significant early time influence on the pressure loading even though that surface is blown out immediately thereafter.

12

4. The final plate deformation shape was fairly repeatable and was more conical than the parabolic shape typical of static tests.

5. The response of air-backed and water-backed plates differed substantially in shape and amplitude. Air-backed plates sustained two to three times the deformation of corresponding water-backed plates. Air-backed plates deformed into a conical shape whereas water-backed plates tended to deform more spherically and some had a center "dimple" caused by hydrodynamic effects.

6. Preliminary scaling relationships for the center deflection of both air- and water-backed plates have been deduced from the data.

7. Plate failures were at the edge for all cases except those in which the charge was near the plate at a stand-off of 1 1/2 plate radii or less. At those near ranges, center failure occurred.

8. Plate failure cannot be predicted accurately by the analytical method of Sewell and Kinney[1] for the load and support conditions investigated here. A more complex analysis appears necessary for the development of a reliable criterion for failure.

9. Rate of pressure decay during venting to the atmosphere through small openings can be estimated well by the analysis method of Proctor[2] for initial pressures in excess of 200 psi.

ACKNOWLEDGMENTS

3 IN. DIAMETER PIPE PLUG USED FOR ARMING THE CHAMBER; SEE FIGURE 3 FOR DETAIL

1/2 IN. THICK SEAMLESS STEEL PIPE WITH 1 IN. HY80 PLATE WELDED ONTO ONE END

37 1/4"

11 3/4"

TEST PLATE CLAMPED INTO PLACE; SEE FIGURE 2 FOR DETAIL
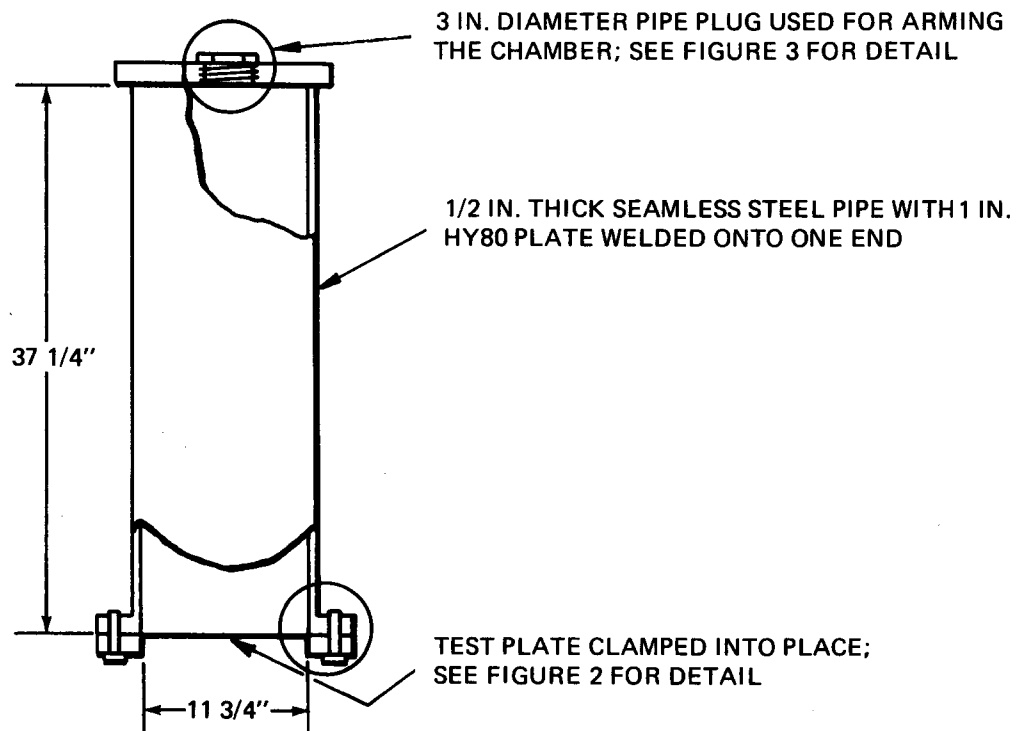
Figure 1 — Explosion Chamber

O-RING GASKET IN GROOVE

ONE (OF 24) 7/8 IN. HIGH STRENGTH BOLTS TIGHTENED TO A TORQUE OF 300 FT-LB

HY-80 STEEL FLANGE WITH FACE MACHINED FLAT AND GROOVED TO INCREASE FRICTIONAL FORCES

TEST PLATE

r = 1/8"

1 1/4"

CLAMPING RING

2 1/2"
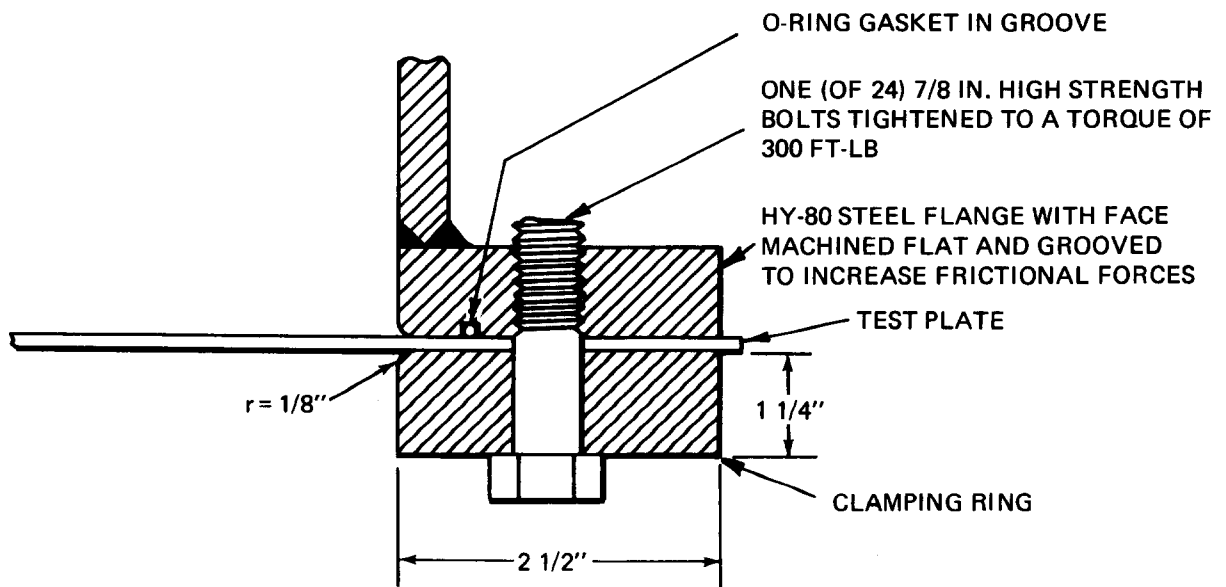
Figure 2 — Test Plate Clamped into Position

14

DETONATOR IS PUSHED THROUGH
THE PIPE PLUG INTO THE PENTOLITE
CHARGE

WOODEN DOWELS SUPPORTING THE
CHARGE CAN BE MOVED TO VARY THE
CHARGE RANGE

3 IN. DIAMETER PIPE PLUG WITH HOLES
BORED TO ACCEPT A DETONATOR AND
TWO DOWELS

STYROFOAM SPACER

PENTOLITE CHARGE TAPED BETWEEN
THE TWO DOWELS
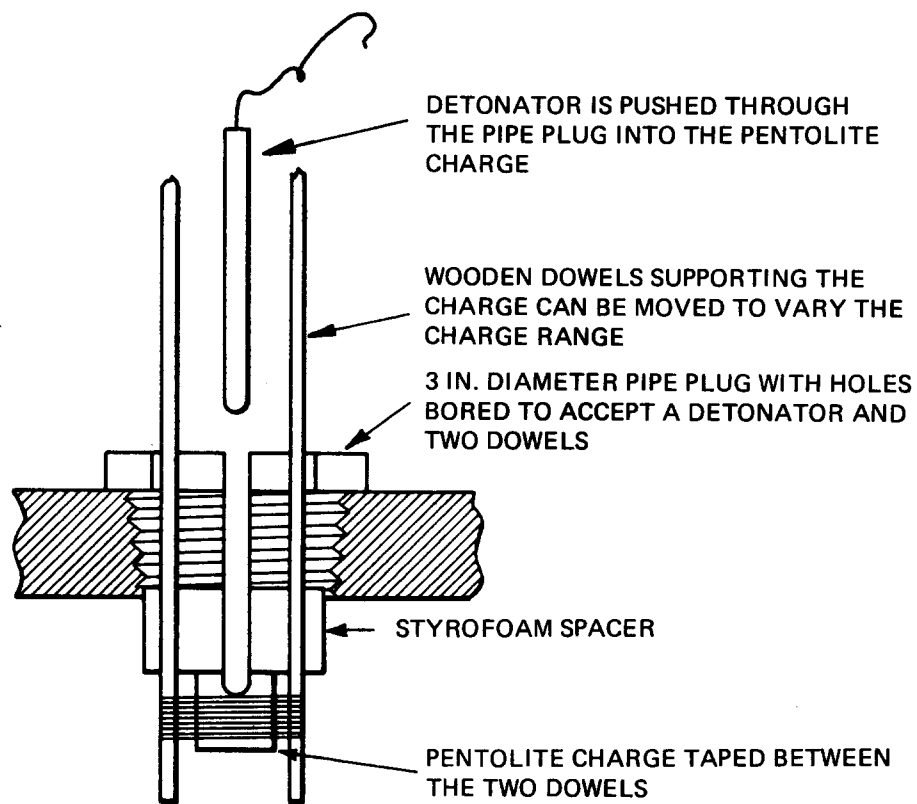
Figure 3 — Arming the Explosion Chamber

RUBBER TIRE SHOCK ABSORBER

AIR TRAPPED UNDER TEST PLATE
REMOVED PRIOR TO TEST
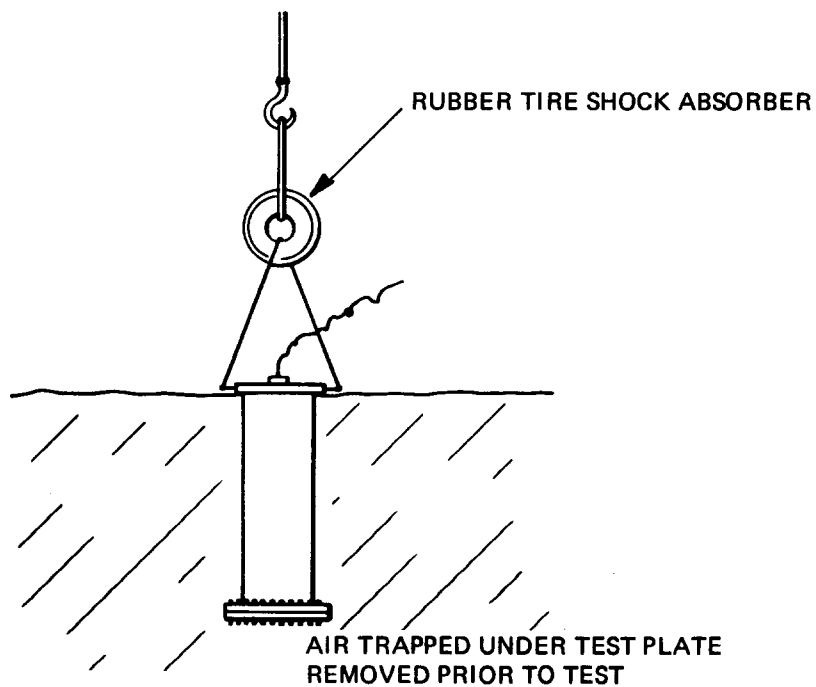
Figure 4 — Explosion Chamber in Test Position for a Water-Backed Test

15

GAGE IN FLANGE;
SEE FIGURE 5b FOR
DETAIL

RIGID PLATE THREADED
TO RECEIVE GAGE AT 3
POSITIONS

← 3″ →

← 5 3/8″ →
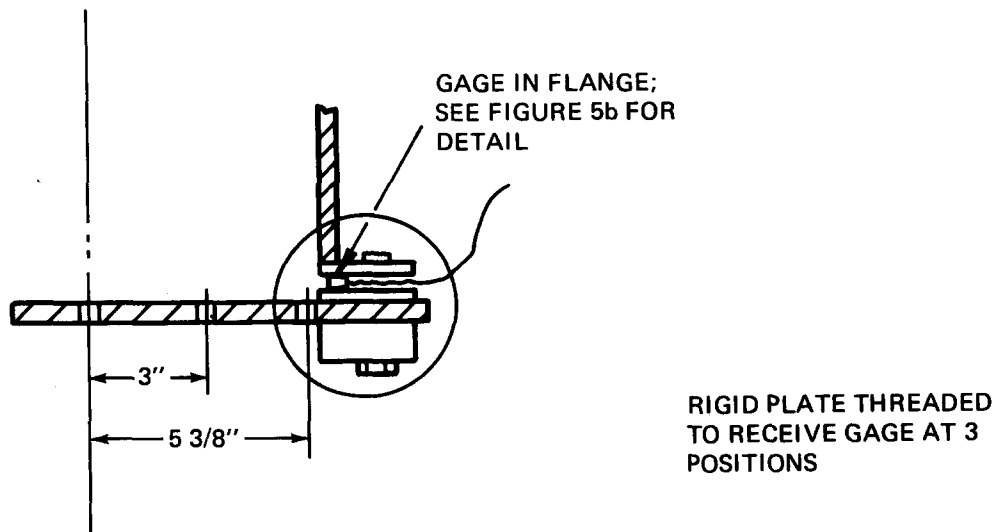
Figure 5a – Gage Positions

THE PRESSURE GAGE
MOUNTED IN ITS HOUSING
AND THREADED INTO THE
FLANGE

THE "RIGID" PLATE

RETAINING RING
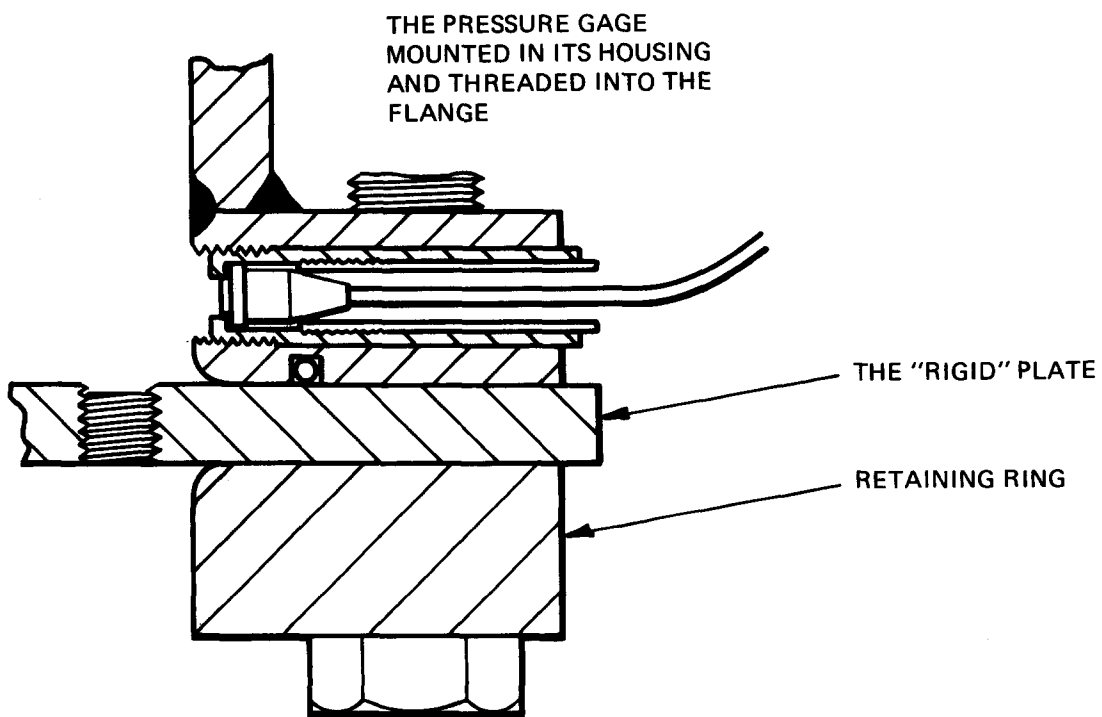
Figure 5b – Details of Gage Geometry

Figure 5 – Pressure Gage Mounted in the Flange

16
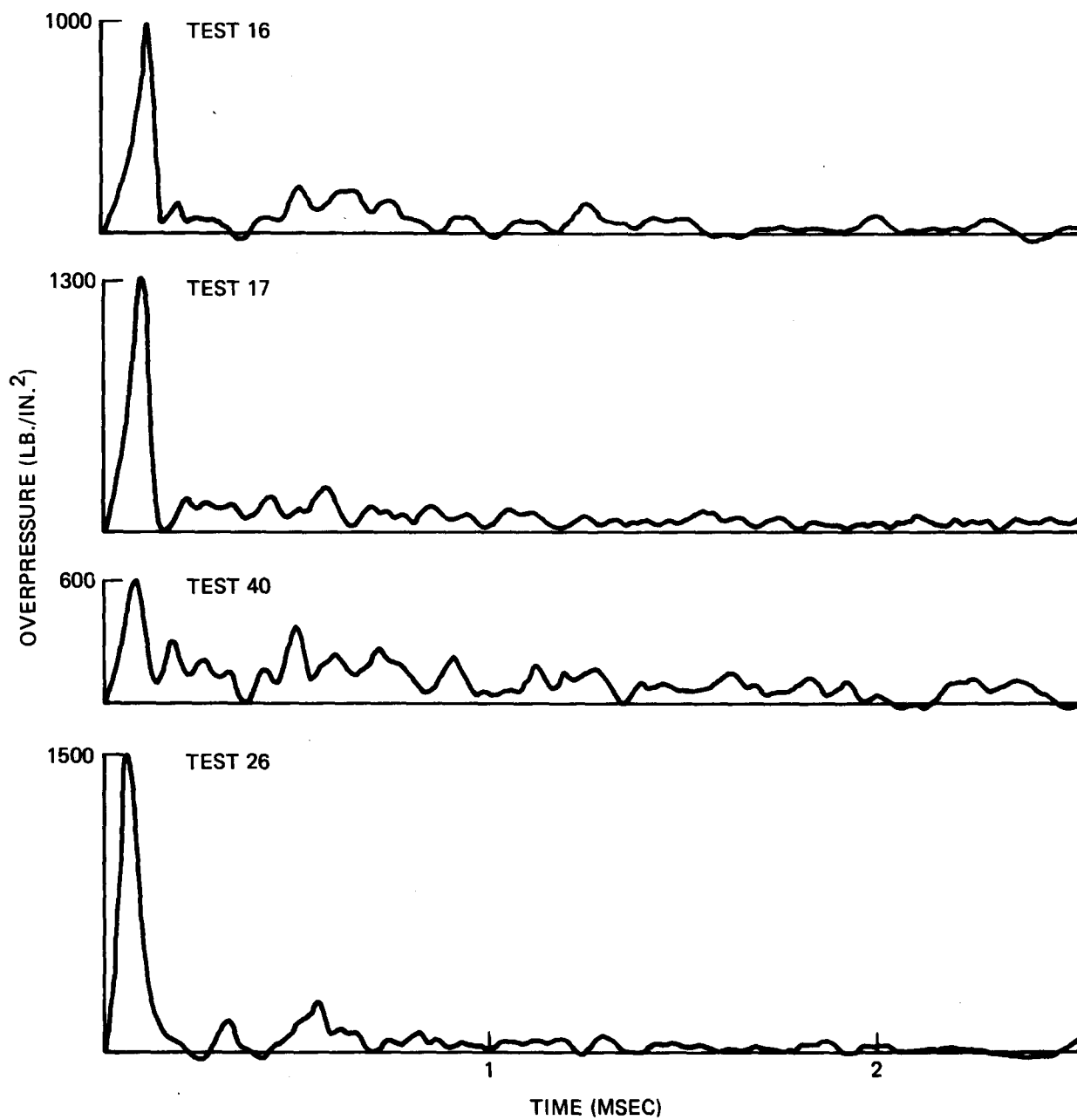
Figure 6 — Pressure Records for 7-Gram Pentolite Charges
(All charges detonated at 35-in. SOD; all pressures measured at the flange)
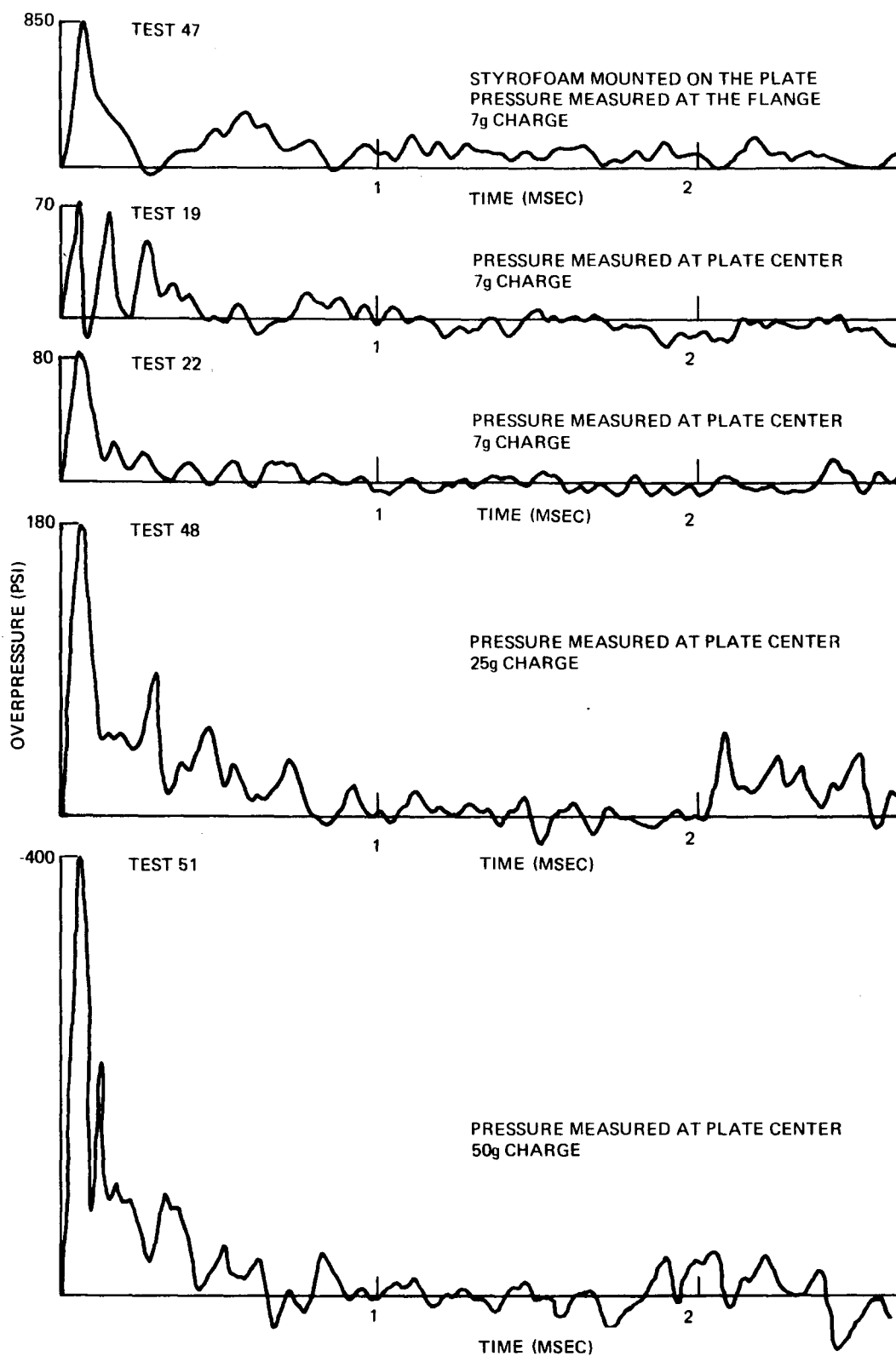
Figure 7 — Pressure Records for Different Gage Positions
(All recorded at 35-in. SOD)
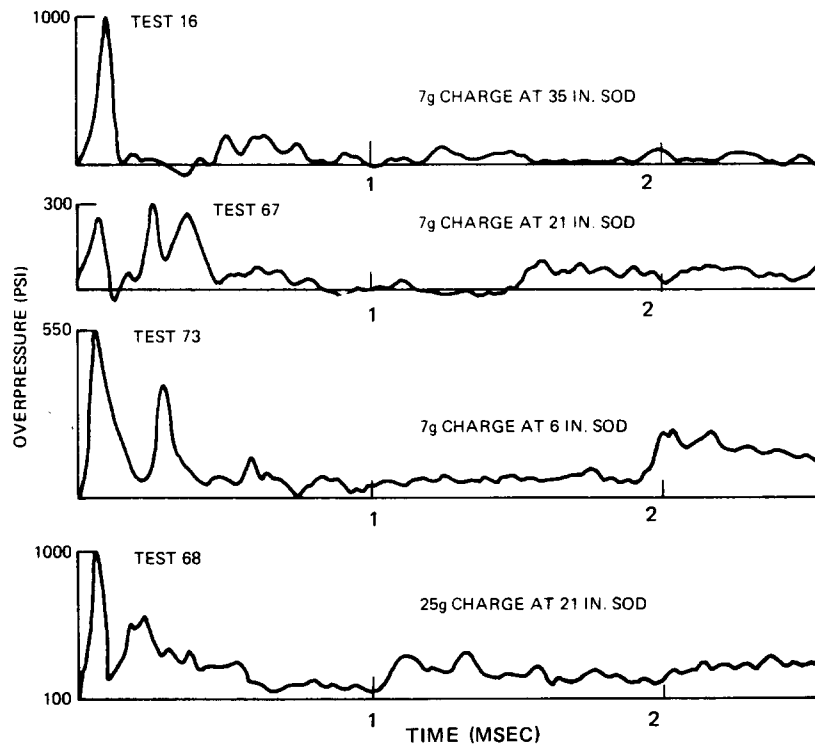
Figure 8 — Pressure Records for Different Charge Positions
(Pressure measured at flange)
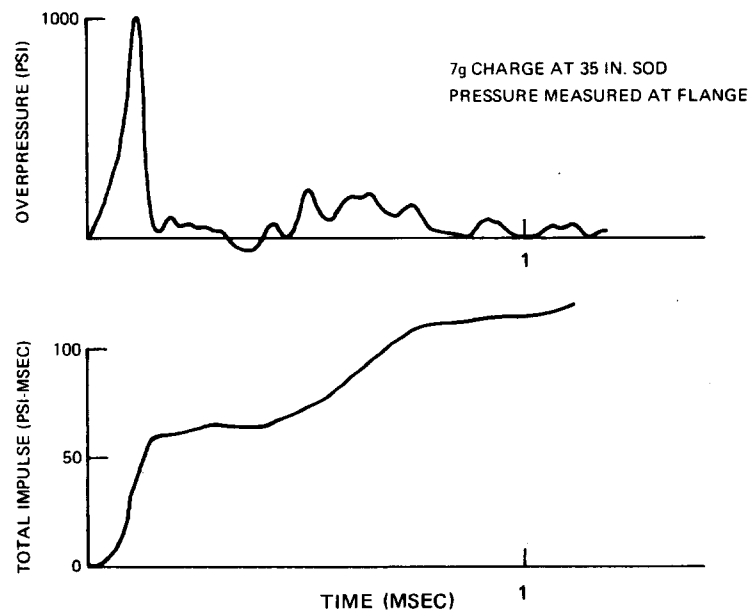
Figure 9 — Pressure Record and Corresponding Impulse Curve, Test 16

19

Figure 10 — Impulse Curves for Tests at Various Standoffs and Charge Weights
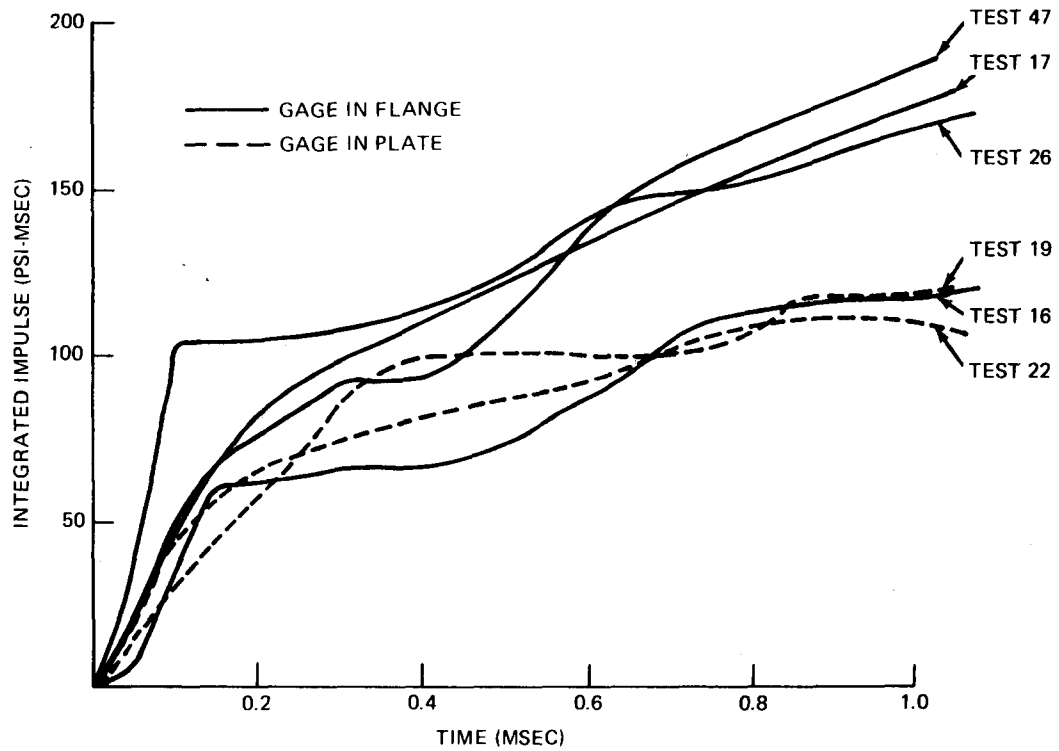
Figure 10a — 7-Gram Charges Detonated at the Full SOD
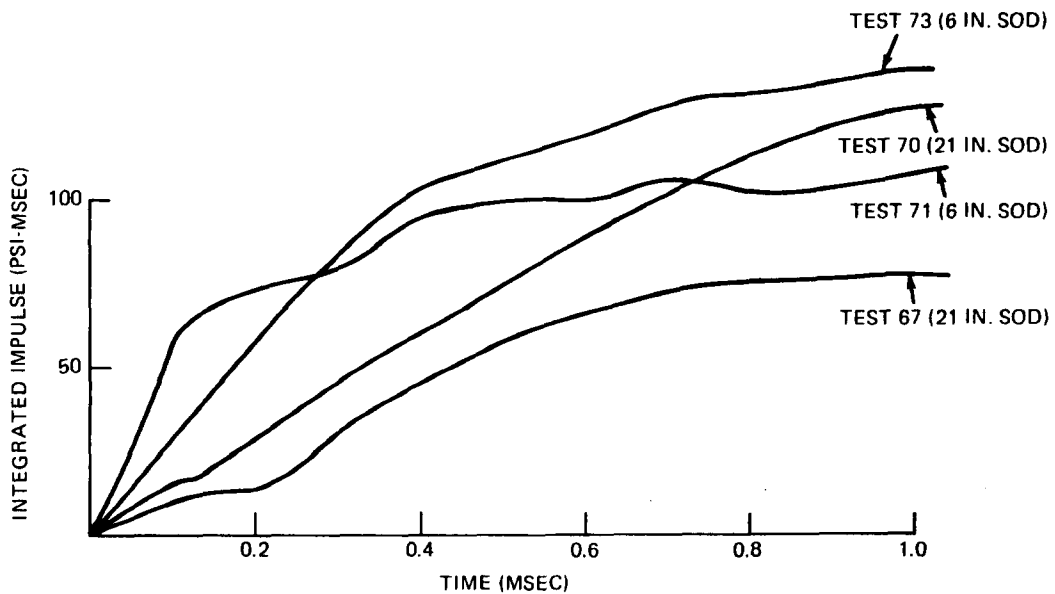
Figure 10b — 7-Gram Charges Detonated at the Shorter SOD

20
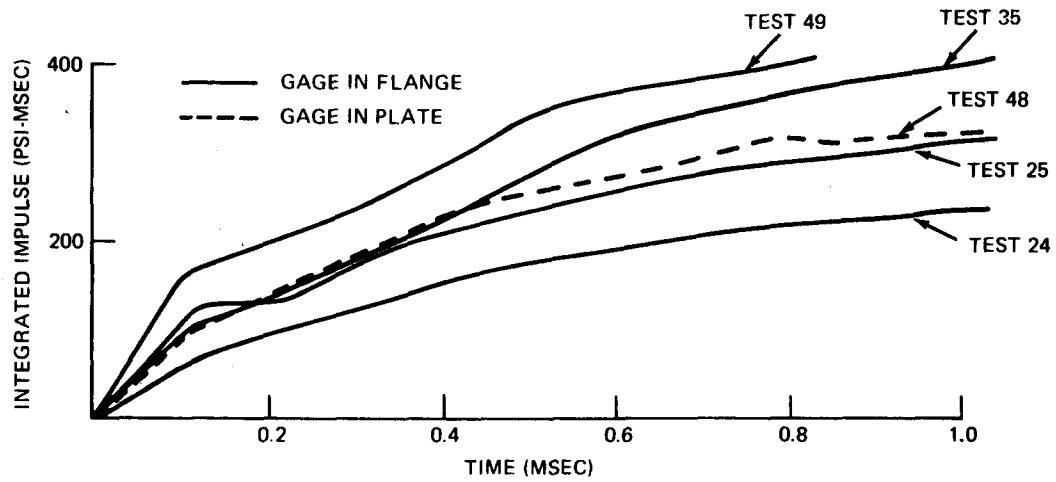
Figure 10 (Cont'd.)

Figure 10c — 25-Gram Charges Detonated at Full SOD
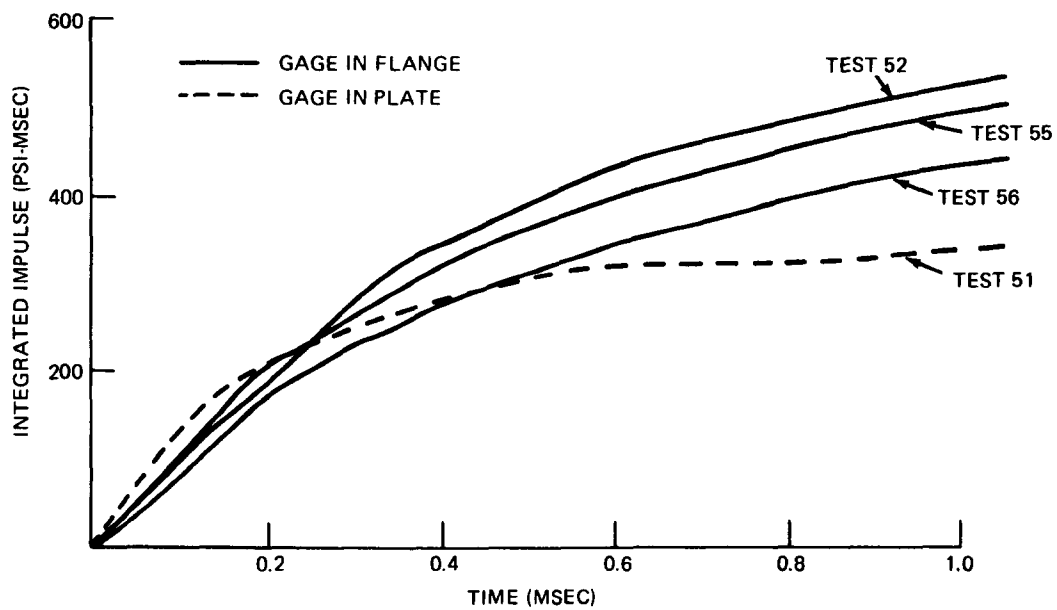
Figure 10d — 50-Gram Charges Detonated at Full SOD

21
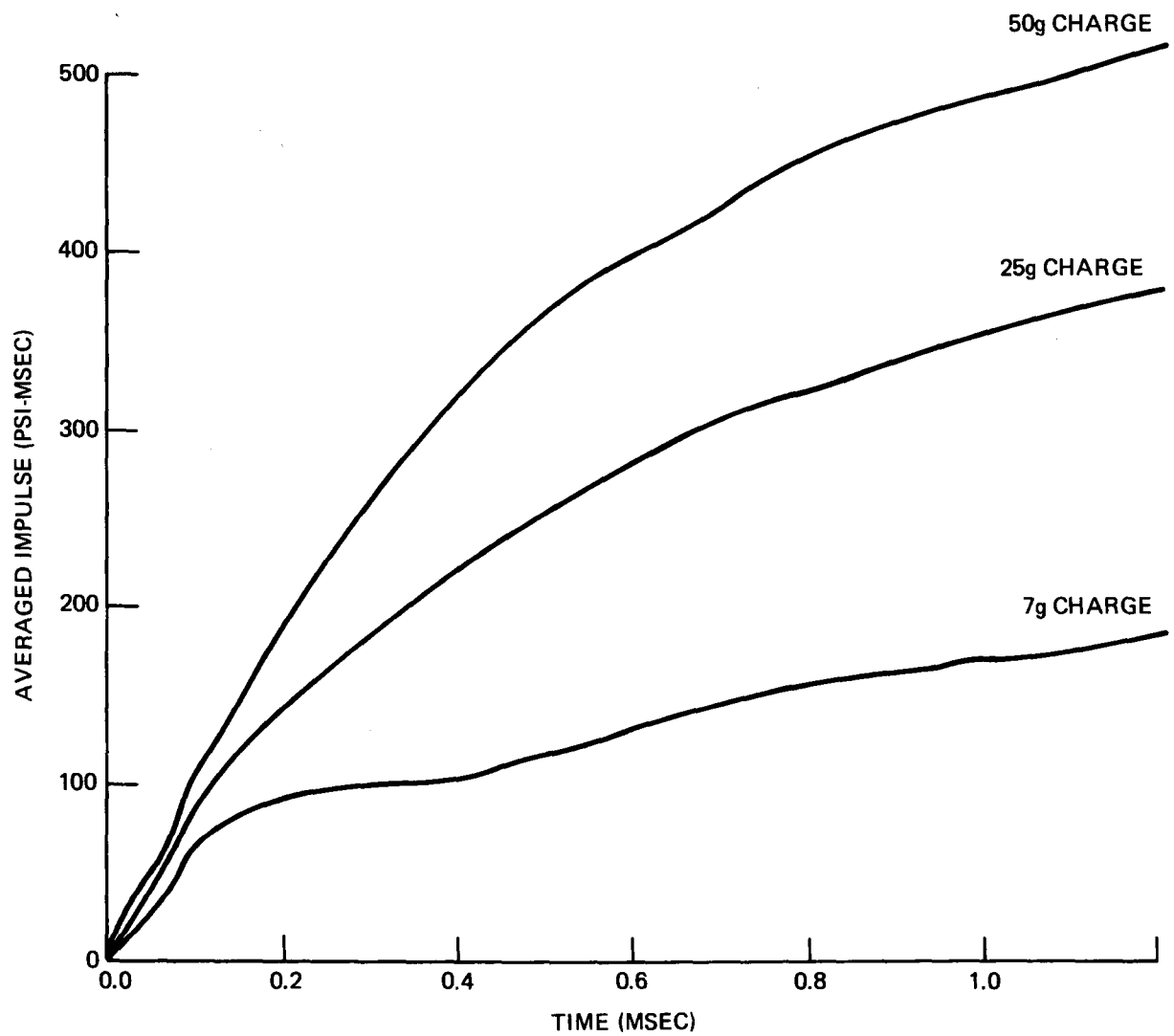
Figure 11 — Averaged Impulse Curves for Different Charge Weights as Measured at the Flange

(Measured at the flange, SOD = 35 in.)

Figure 12 — Final Deformed Shapes of the Plates

(Tests at 35-in. SOD were conducted with 37-in. chamber and those at 16-in. SOD with 18-in. chamber)

TEST NO.	CHARGE WT. (GM)
1,9	7
2,107	15
3,6,106	25
4	50
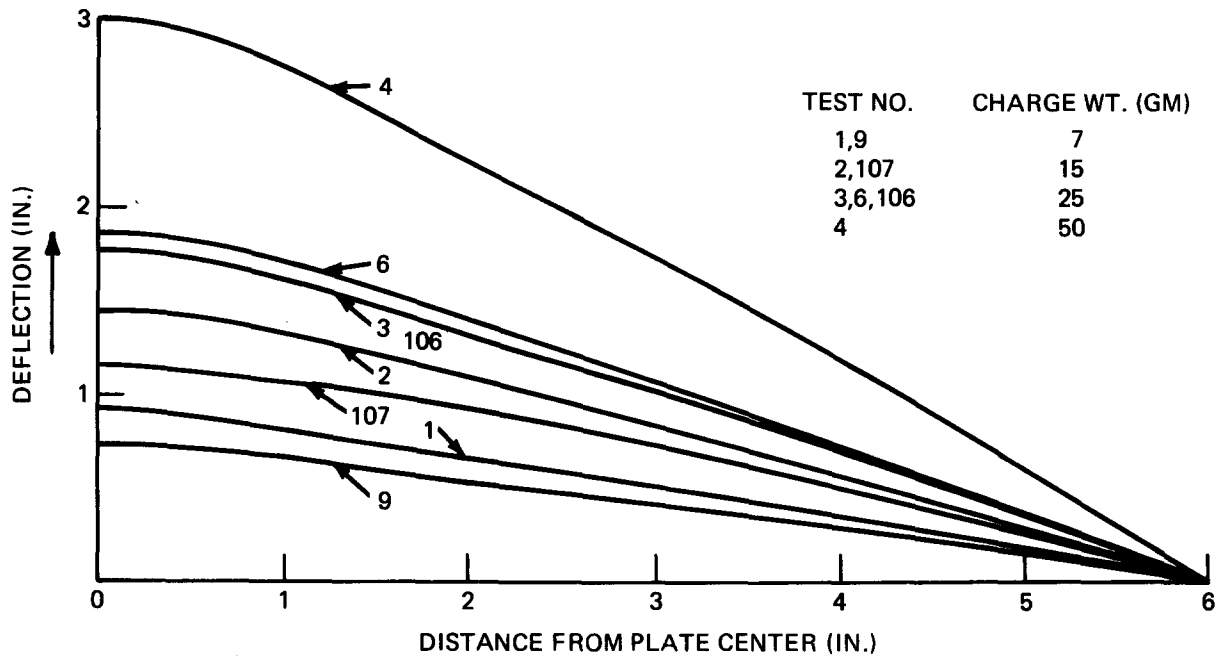
Figure 12a — 1/16-Inch Medium Steel, Air Backed, SOD = 35 Inches

TEST NO.	CHARGE WT. (GM)
7	50
8	100
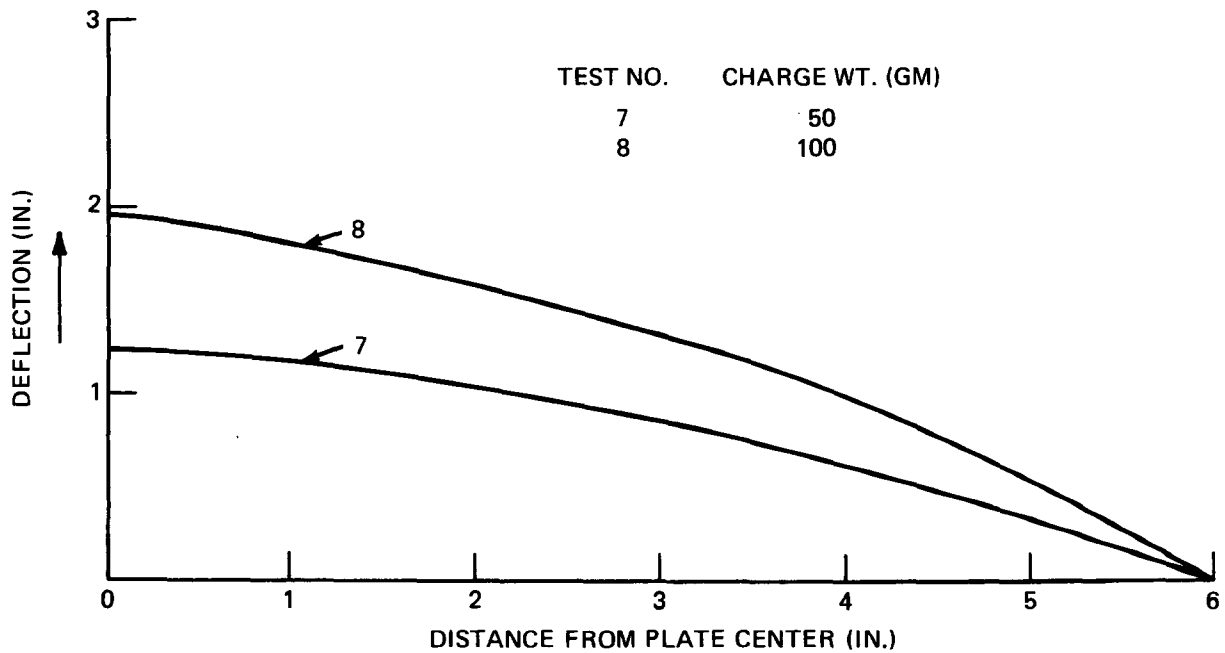
Figure 12b — 1/16-Inch Medium Steel, Water Backed, SOD = 35 Inches

23
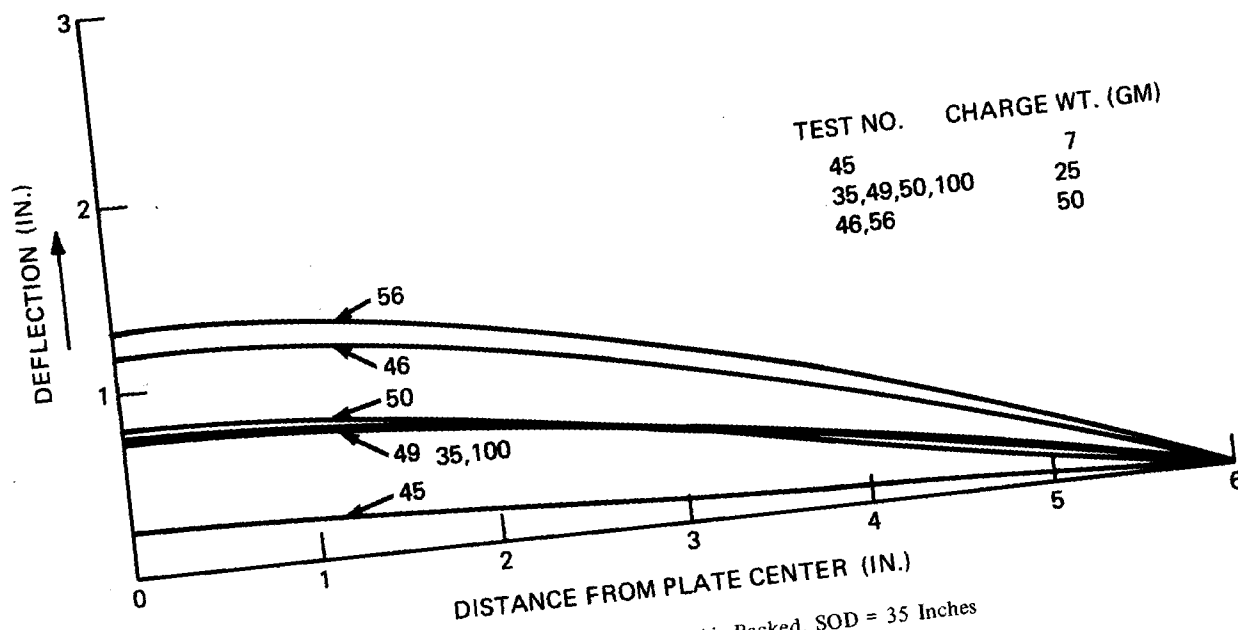
Figure 12 (Cont'd.)

Figure 12c — 1/8-Inch Medium Steel, Air Backed, SOD = 35 Inches
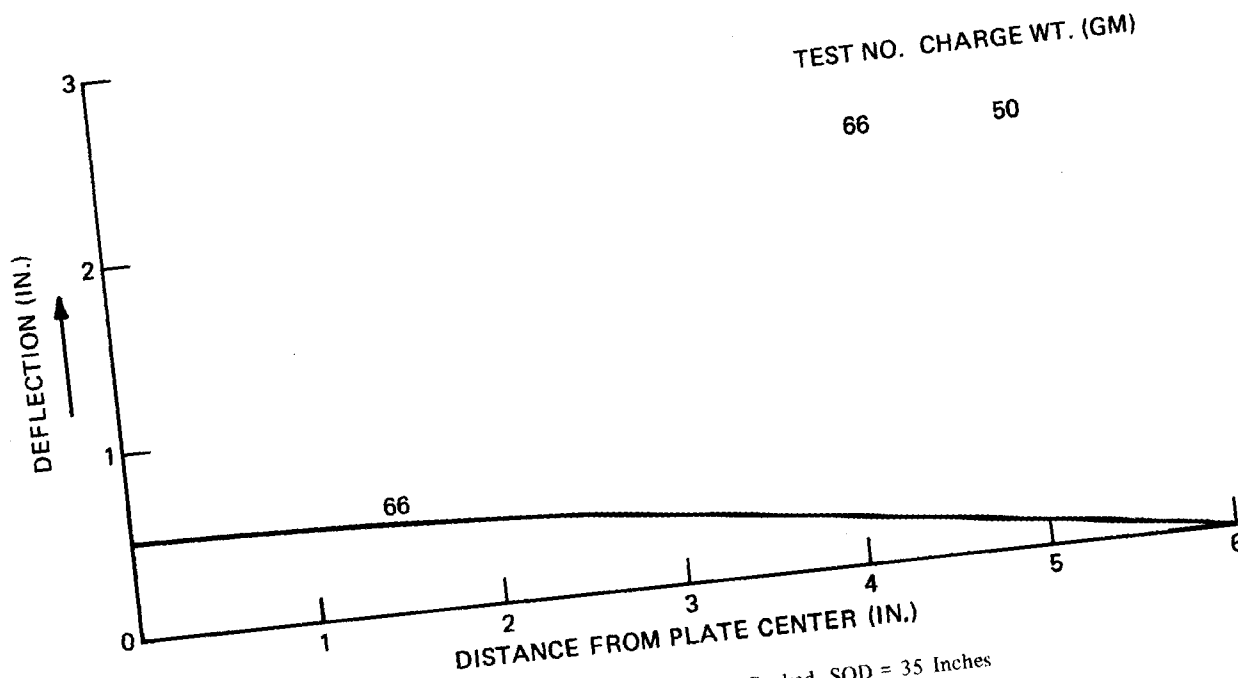
Figure 12d — 1/8-Inch Medium Steel, Water Backed, SOD = 35 Inches

Figure 12 (Cont'd.)

TEST NO.	CHARGE WT. (GM.)
26	7
28	15

DISTANCE FROM PLATE CENTER (IN.)

Figure 12e – 1/16-Inch Aluminum, Air Backed, SOD = 35 Inches

TEST NO.	CHARGE WT. (GM)
57	7
58	15
59	25
61	32
62	40

DISTANCE FROM PLATE CENTER (IN.)

Figure 12f – 1/16-Inch Aluminum, Water Backed, SOD = 35 Inches
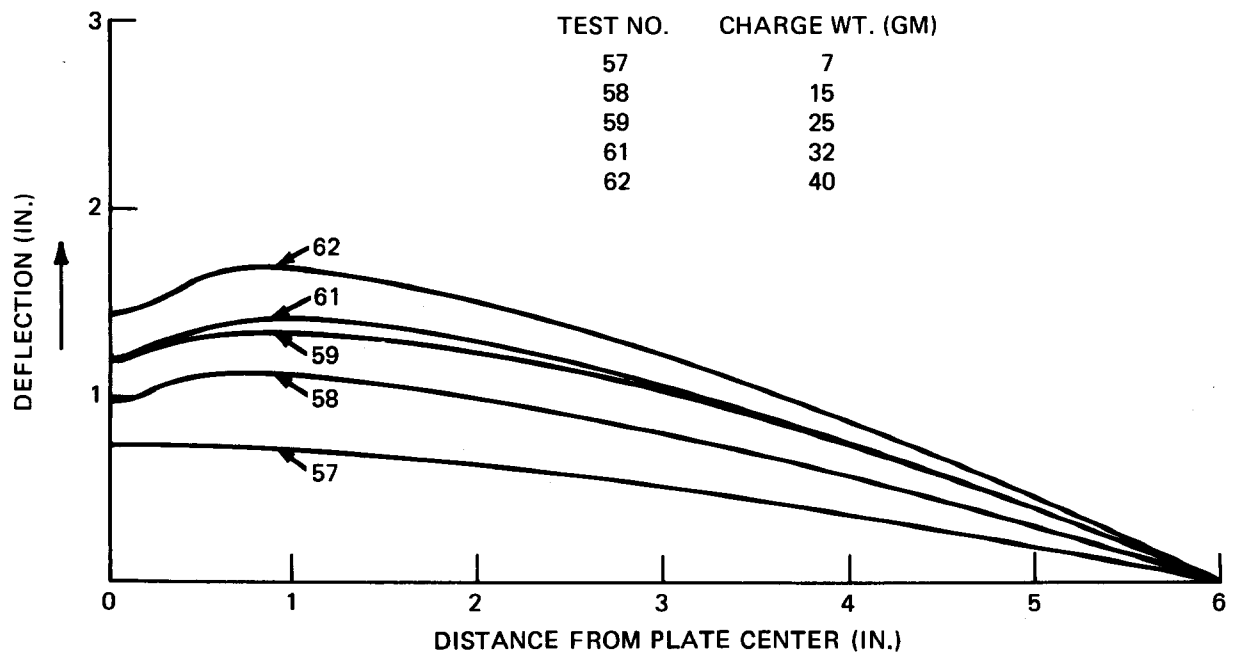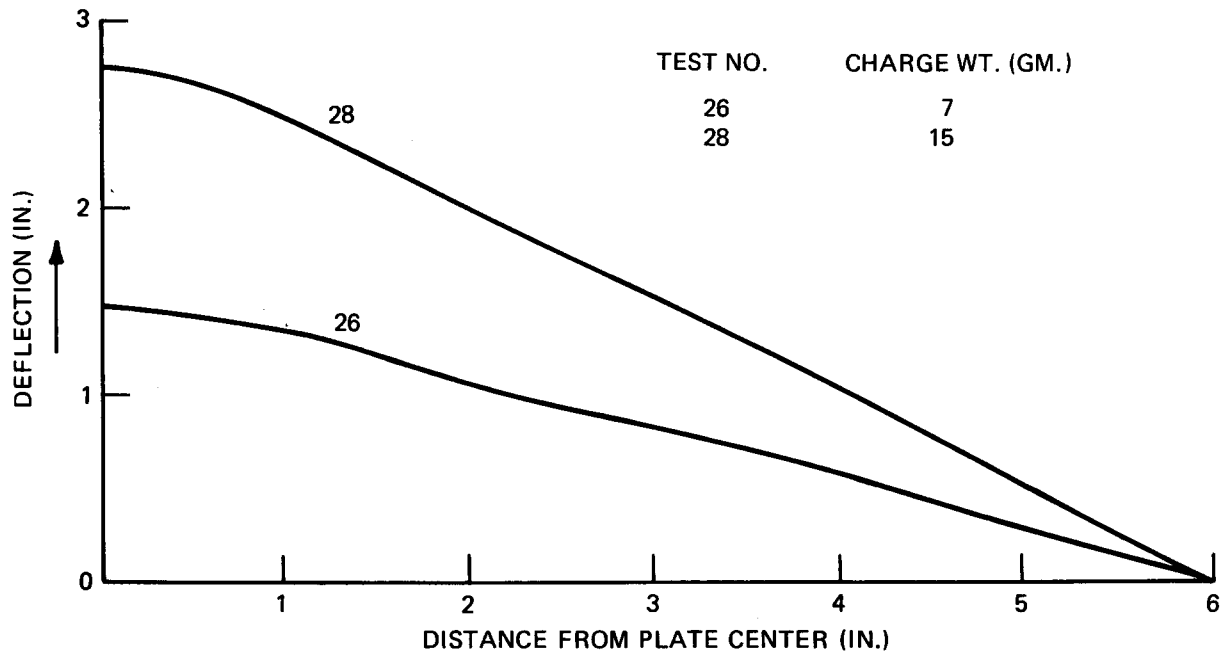
Figure 12 (Cont'd.)

Figure 12g — 1/8-Inch Aluminum, Air Backed, SOD = 35 Inches
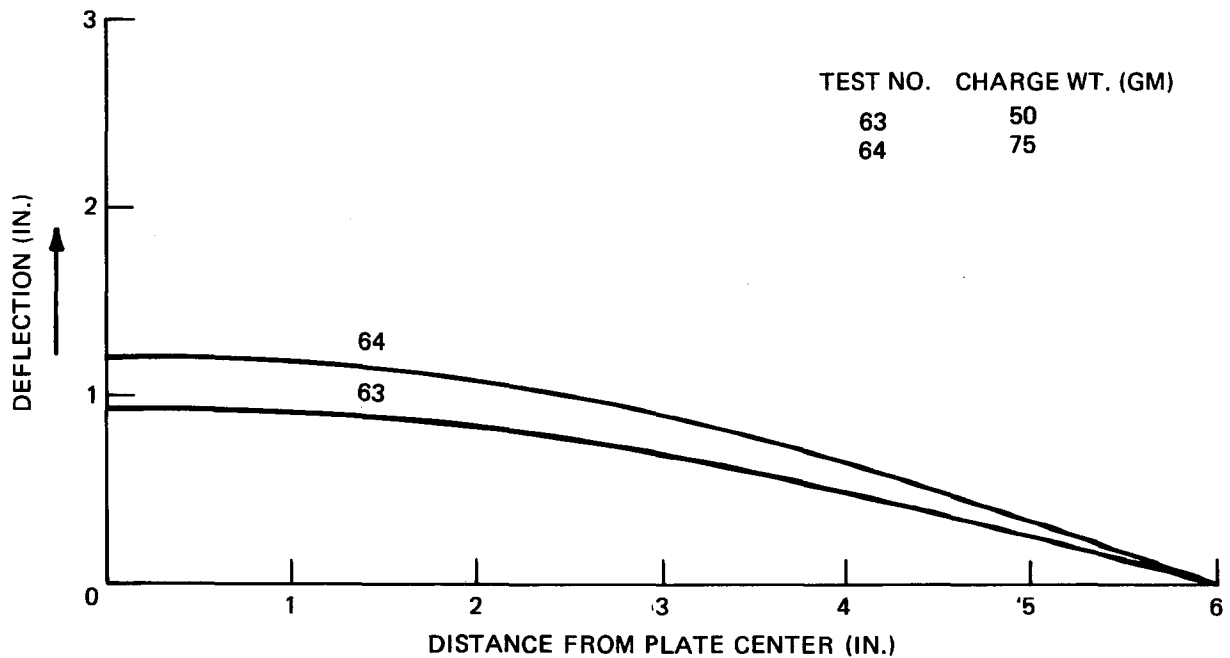
Figure 12h — 1/8-Inch Aluminum, Water Backed, SOD = 35 Inches
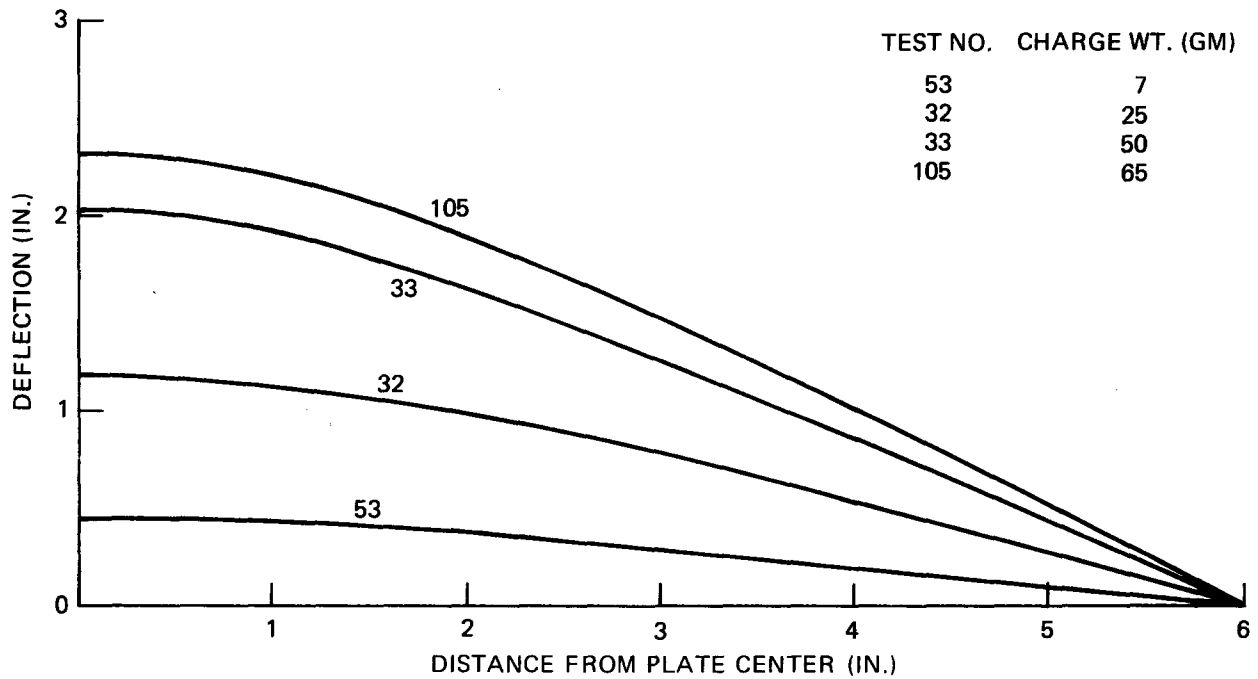
Figure 12i – 3/16-Inch Aluminum, Air Backed, SOD = 35 Inches
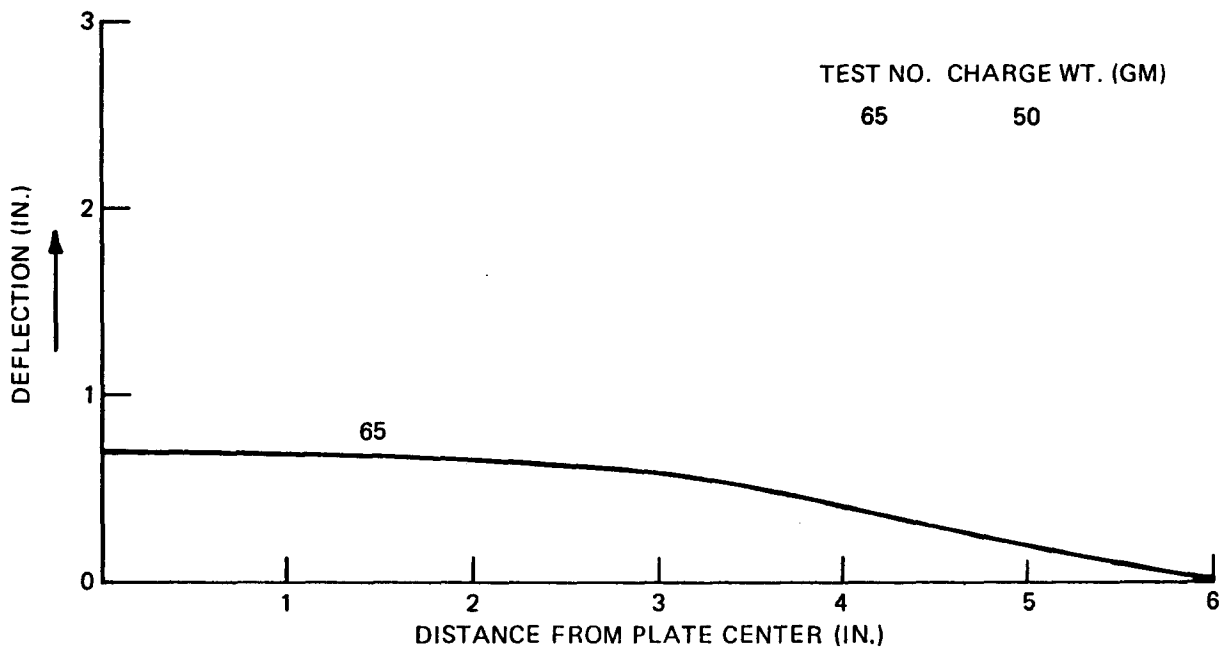
Figure 12j – 3/16-Inch Aluminum, Water Backed, SOD = 35 Inches

27
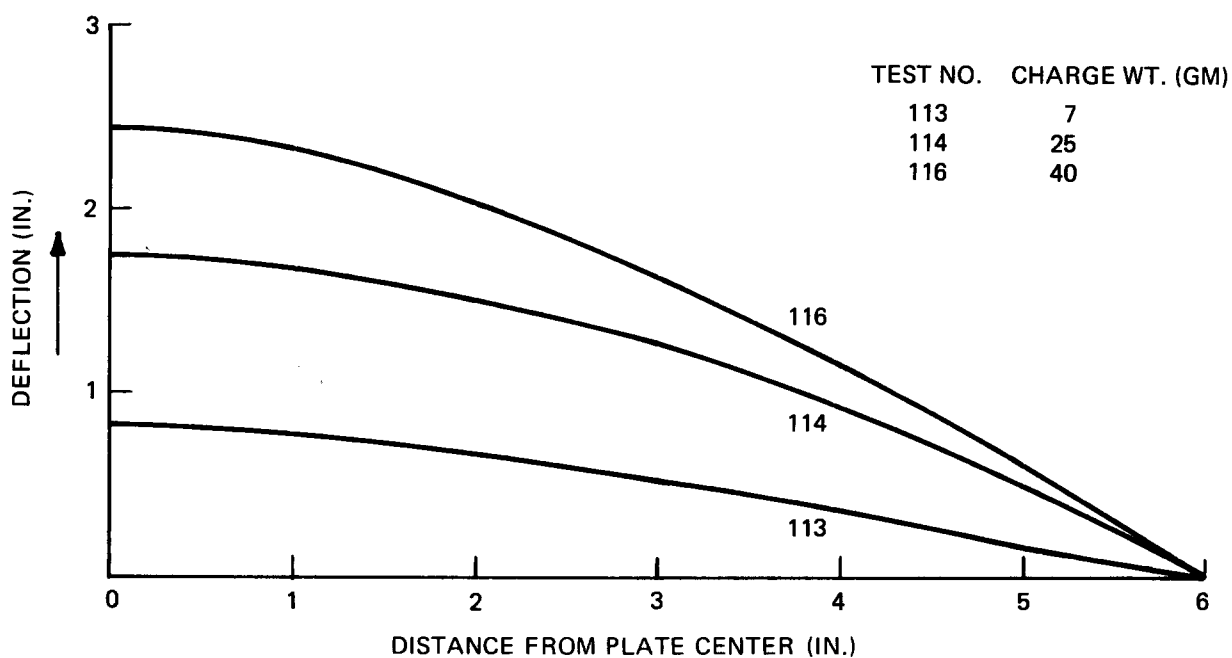
Figure 12k – 1/16-Inch Medium Steel, Air Backed, SOD = 16 Inches
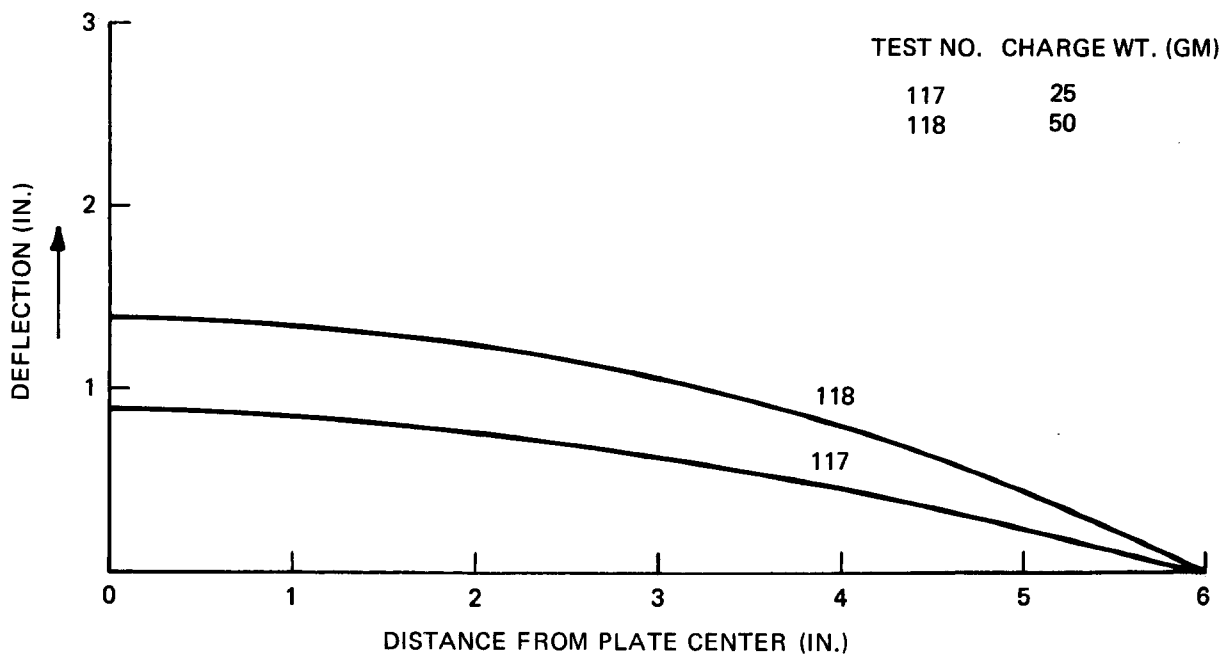
Figure 12l – 1/8-Inch Medium Steel, Air Backed, SOD = 16 Inches

28

TEST NO.	PLATE	CHARGE WT. (GM)
119	1/16" A1	7
122	1/8" A1	15
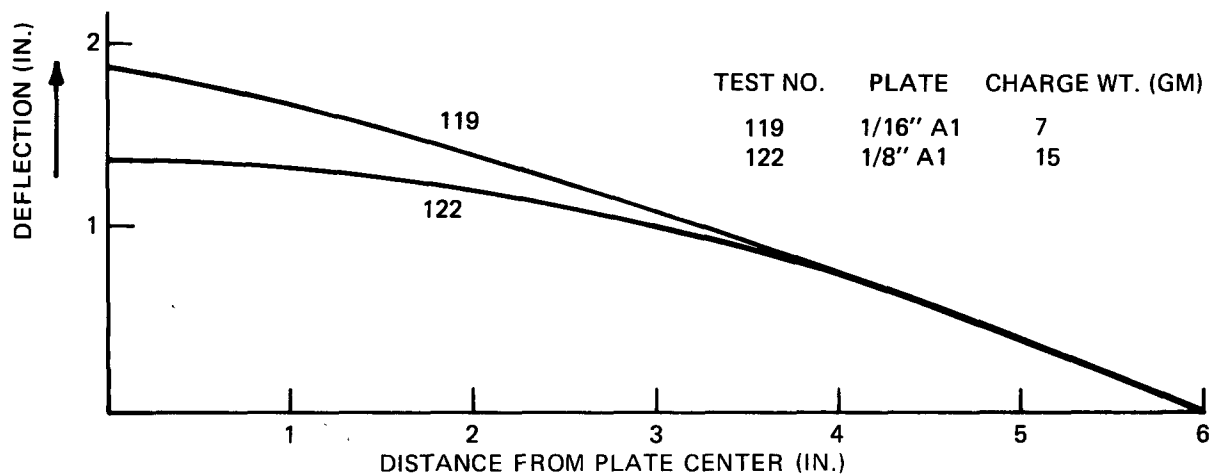
Figure 12m — 1/16- and 1/8-Inch Aluminum, Air Backed, SOD = 16 Inches

TEST NO.	CHARGE WT. (GM)
123	25
124	40
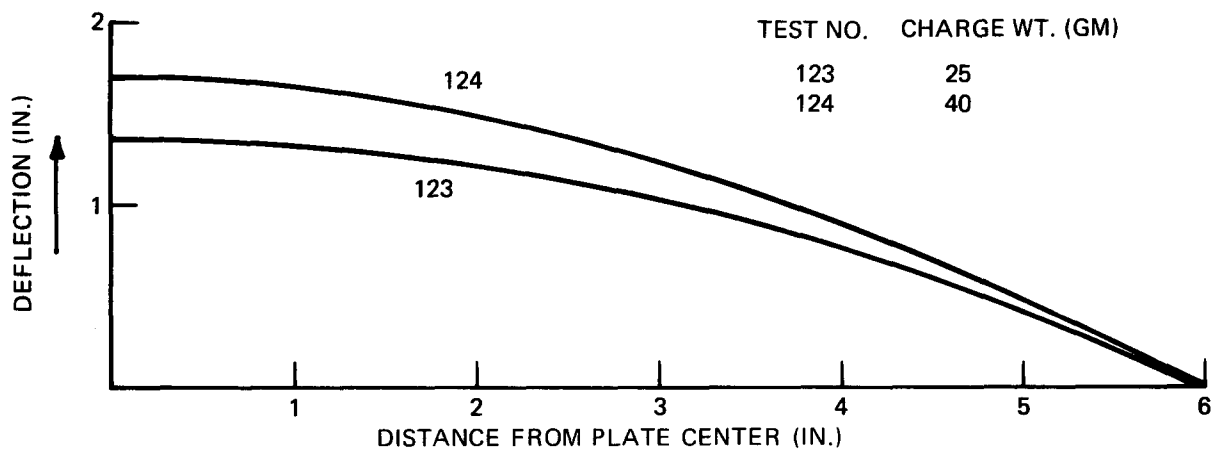
Figure 12n — 3/16-Inch Aluminum, Air Backed, SOD = 16 Inches

TEST NO.	CHARGE WT(GM)	SOD (IN.)
73	7	6
74	25	6
67	7	21
68	25	21
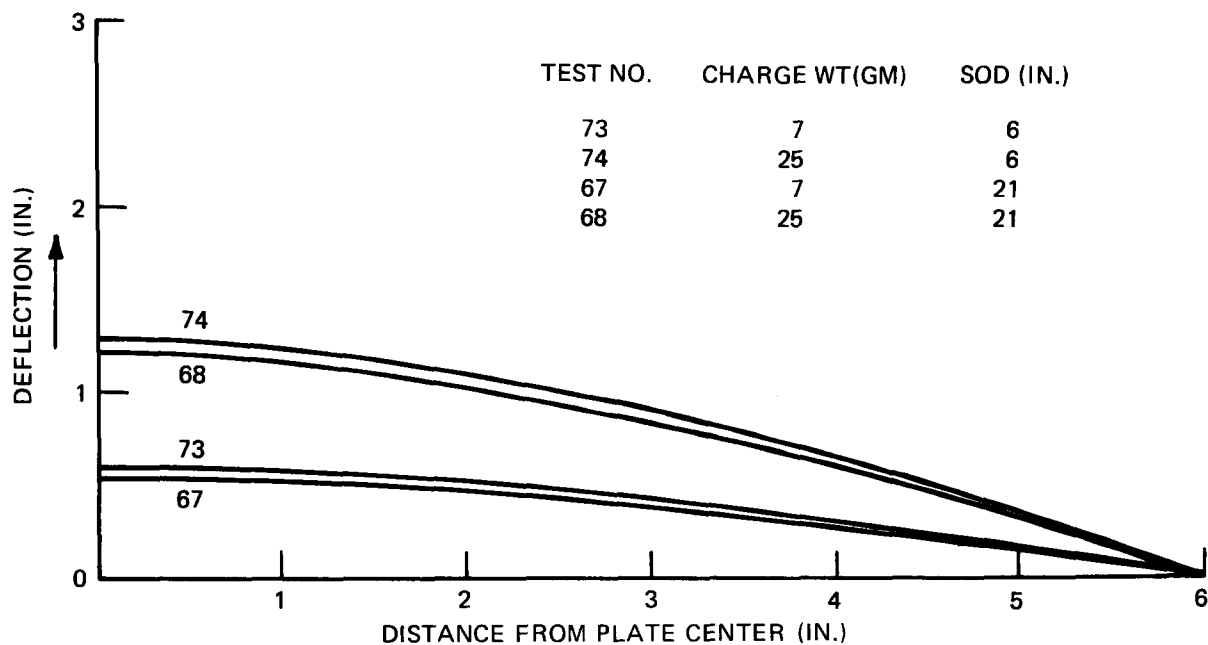
Figure 12o — 3/16-Inch Medium Steel, Air Backed, SOD = 21 Inches and 6 Inches

29

Figure 13 – Typical Deformed and Ruptured Plates

TEST 4, 50-GRAM CHARGE
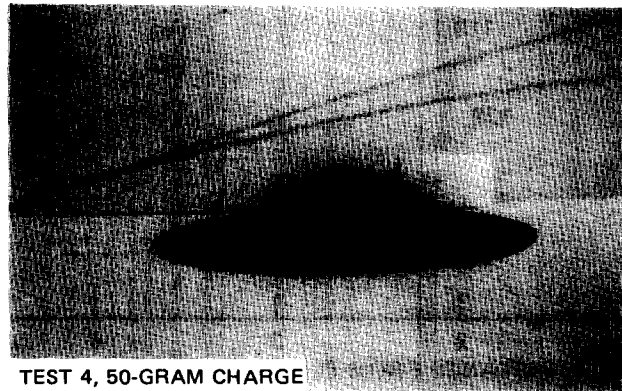
Figure 13a – Air-Backed 1/16-Inch Medium Steel Plate
near Point of Rupture

TEST 7, 50-GRAM CHARGE

Figure 13b – Water-Backed 1/16-Inch Medium Steel Plate
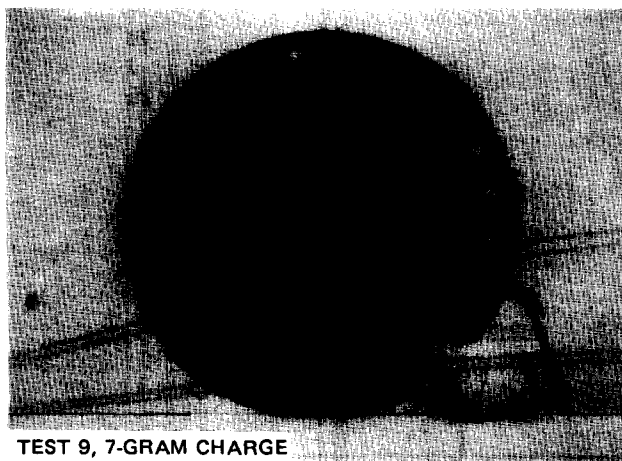
TEST 9, 7-GRAM CHARGE

Figure 13c – Air-Backed 1/16-Inch Steel Plate with Strain Gages
(The center gage flew off during the test and the adhesive
cracked under the other gages)

30
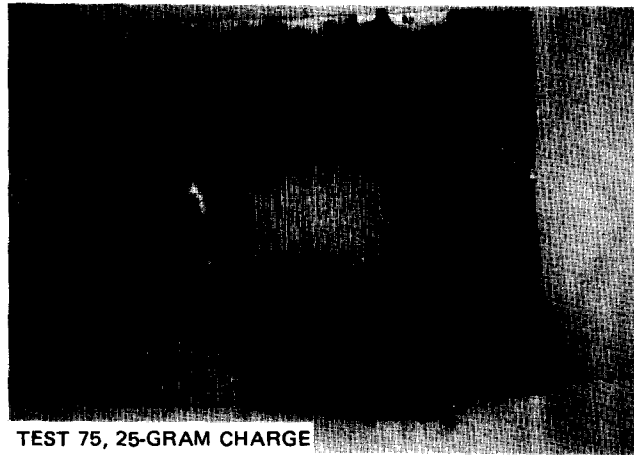
TEST 75, 25-GRAM CHARGE

Figure 13d – Center Rupture of a 1/16-Inch Aluminum, Air-Backed Plate
(Charge only 6 in. from the plate)
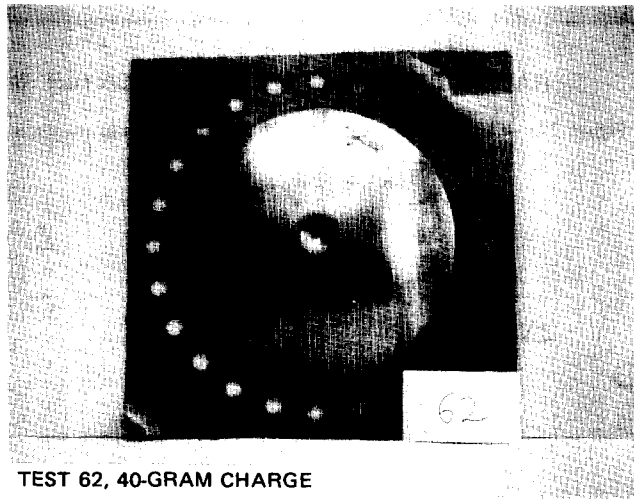
TEST 62, 40-GRAM CHARGE

Figure 13e – Water-Backed 1/16-Inch Aluminum Plate Very Near Failure
(Note the pronounced dimple at the center)
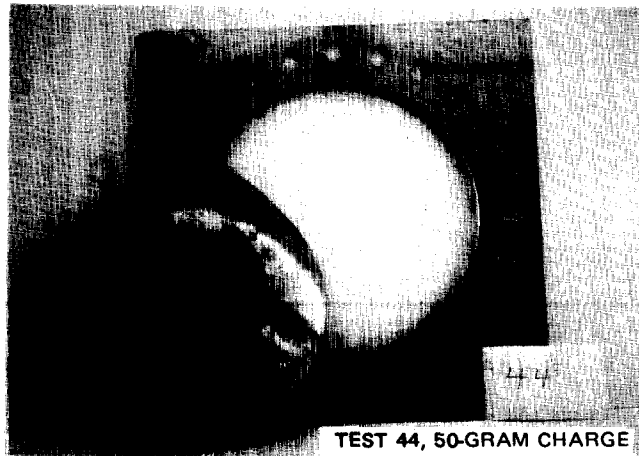
TEST 44, 50-GRAM CHARGE

Figure 13f – Edge Failure of a 1/8-Inch Aluminum, Air-Backed Plate
(All plates with charge at opposite end of chamber failed
in this way)

31
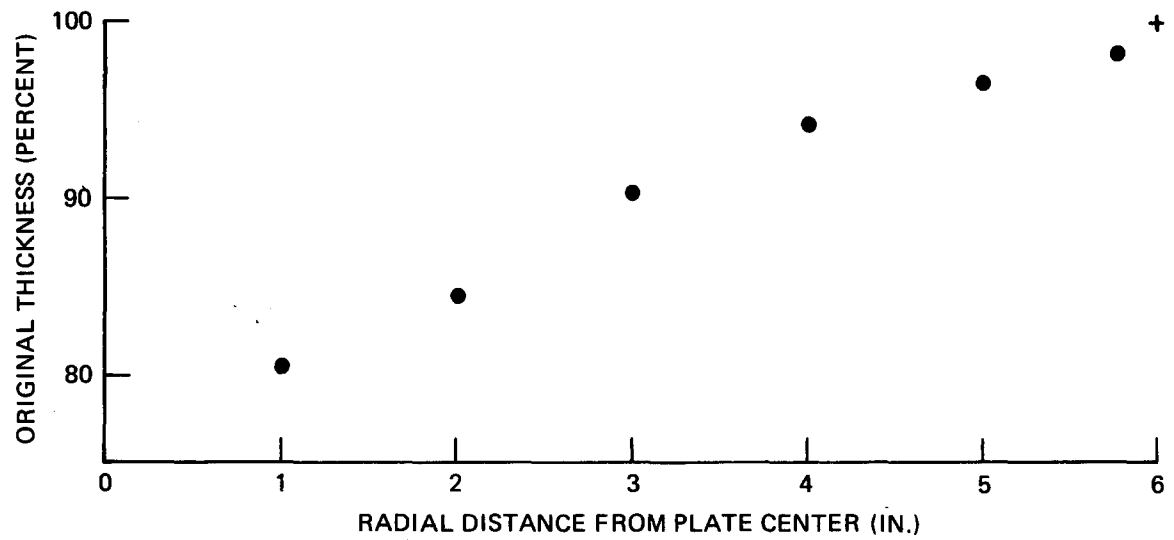
Figure 14a — Final Thickness across a 1/8-Inch Aluminum Plate
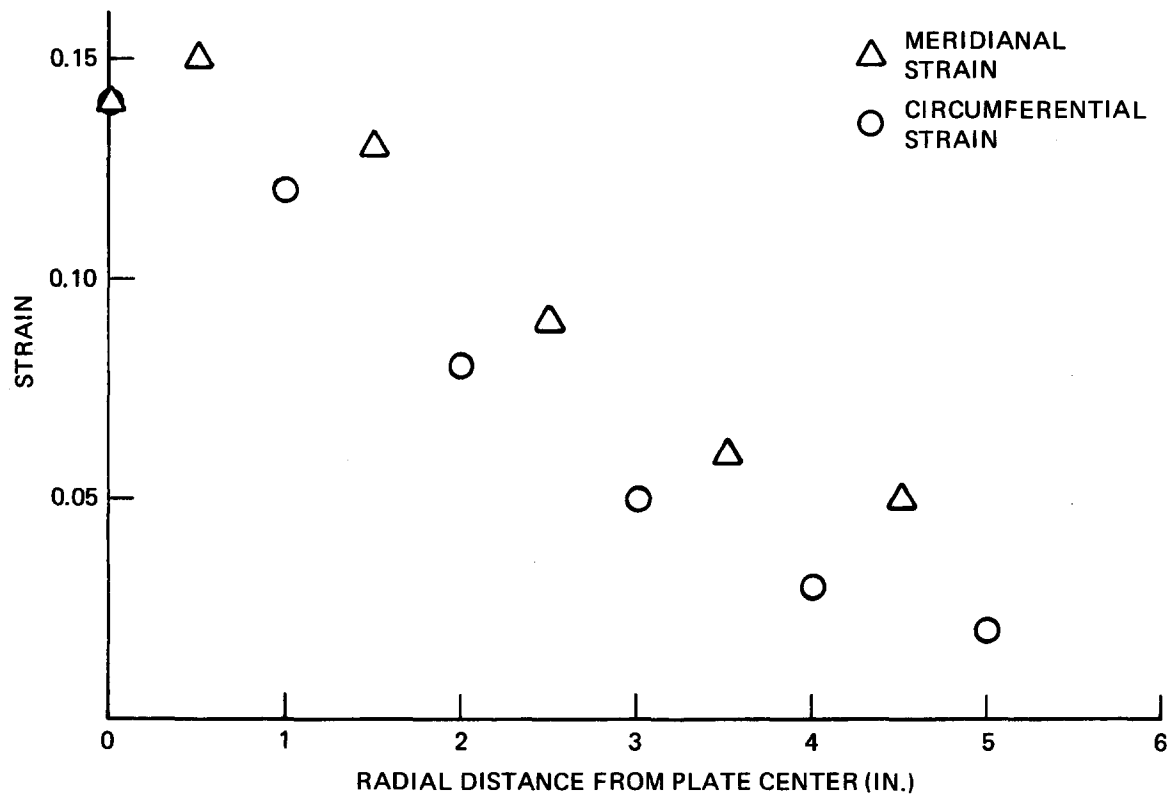
Figure 14b — Final Strains across a 1/8-Inch Aluminum Plate

Figure 14 — Thickness and Strains across an Air-Backed 1/8-Inch Aluminum Plate
Explosively Deformed to a 2.40-Inch Center Deflection (Test 37)

32

Figure 15 — Strain Gage Records for Explosively Loaded Medium Steel Plates

(Strain gage locations are identified only once for each gage number)

865 PSI

1 (MSEC)

PRESSURE GAGE
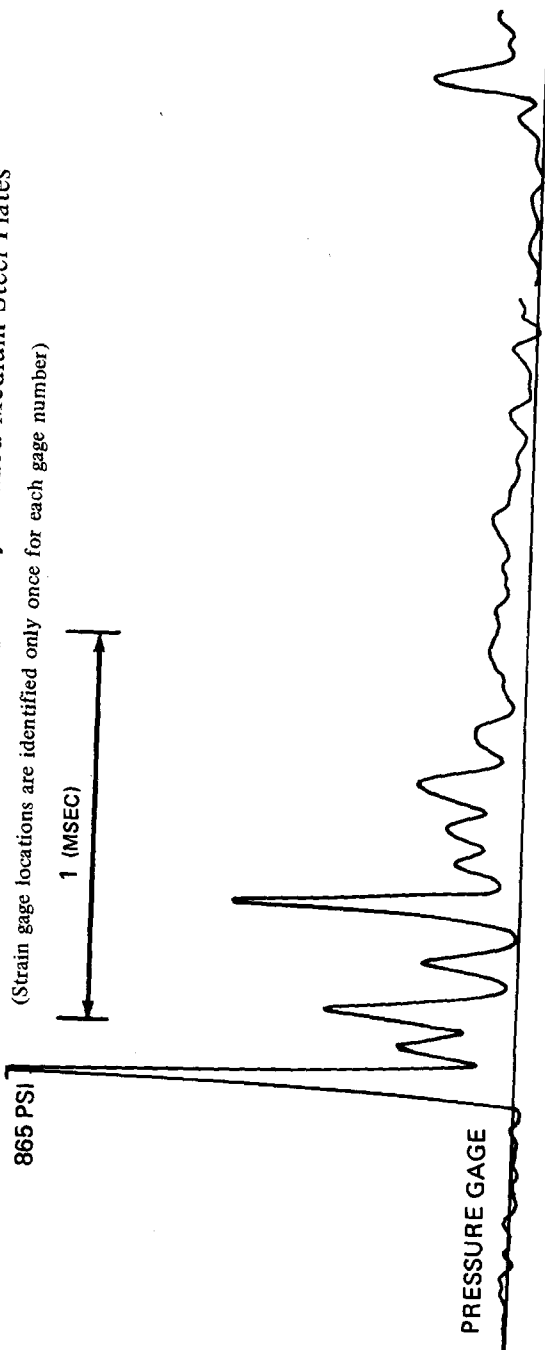
STRAIN GAGE 1 (CENTER OF PLATE)

0.0051 IN/IN

STRAIN GAGE 2 (RADIALLY ALIGNED AT r = 3 IN.)

0.0025 IN/IN

STRAIN GAGE 3 (CIRCUMFERENTIALLY ALIGNED AT r = 3 IN.)

0.0054 IN/IN

Figure 15a — High-Speed Playback of Test 98

(The 1/8-inch steel plate was loaded by a 7-g Pentolite charge detonated at the 35-in. SOD. The resulting permanent deflection at the plate center was 0.25 in.)
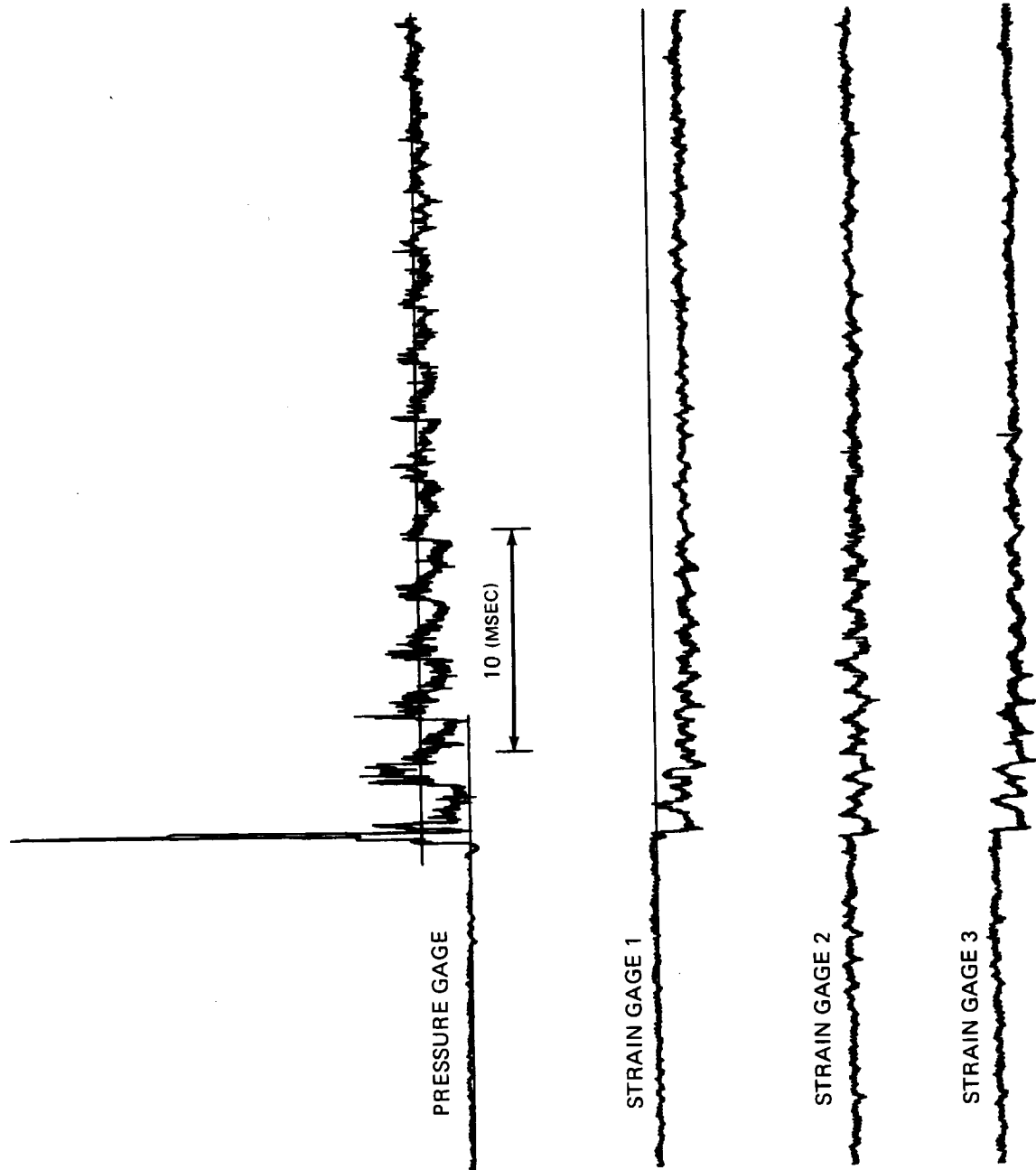
Figure 15b — Slow-Speed Playback of Test 98

PRESSURE GAGE

10 (MSEC)

STRAIN GAGE 1

STRAIN GAGE 2

STRAIN GAGE 3
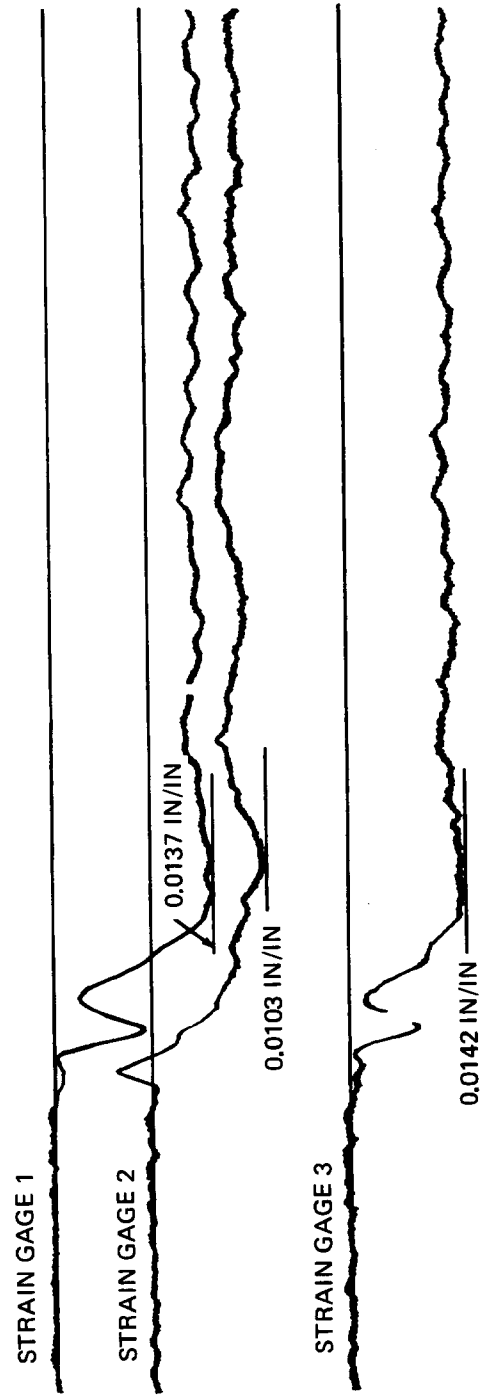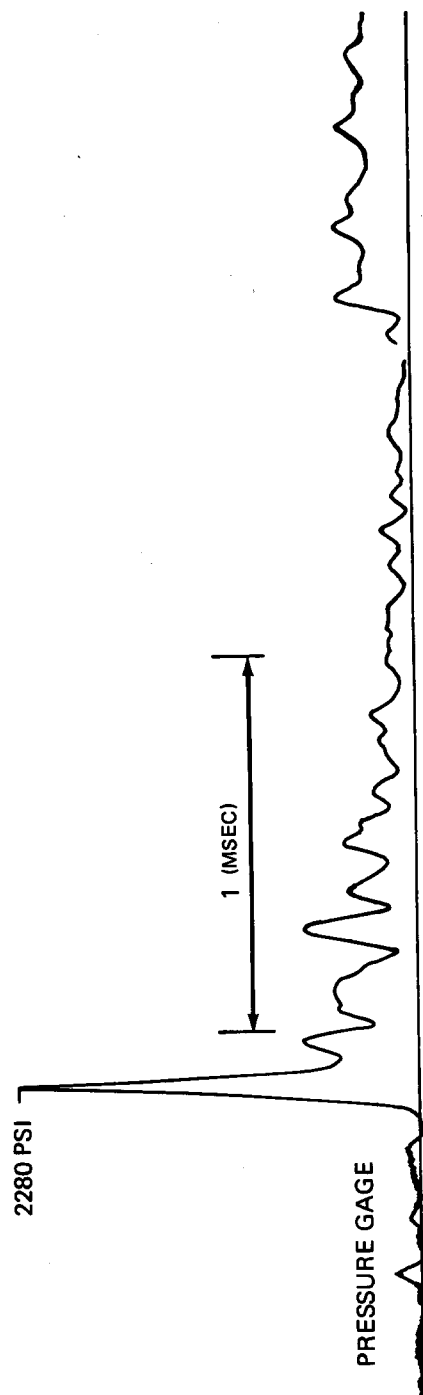
Figure 15c — High-Speed Playback of Test 100

(The 1/8-in. steel plate was loaded by a 25-g Pentolite charge detonated at the 35-in. SOD. The resulting permanent deflection at the plate center was 0.72 in.)

35

PRESSURE GAGE

10 (MSEC)

STRAIN GAGE 1

STRAIN GAGE 2

STRAIN GAGE 3
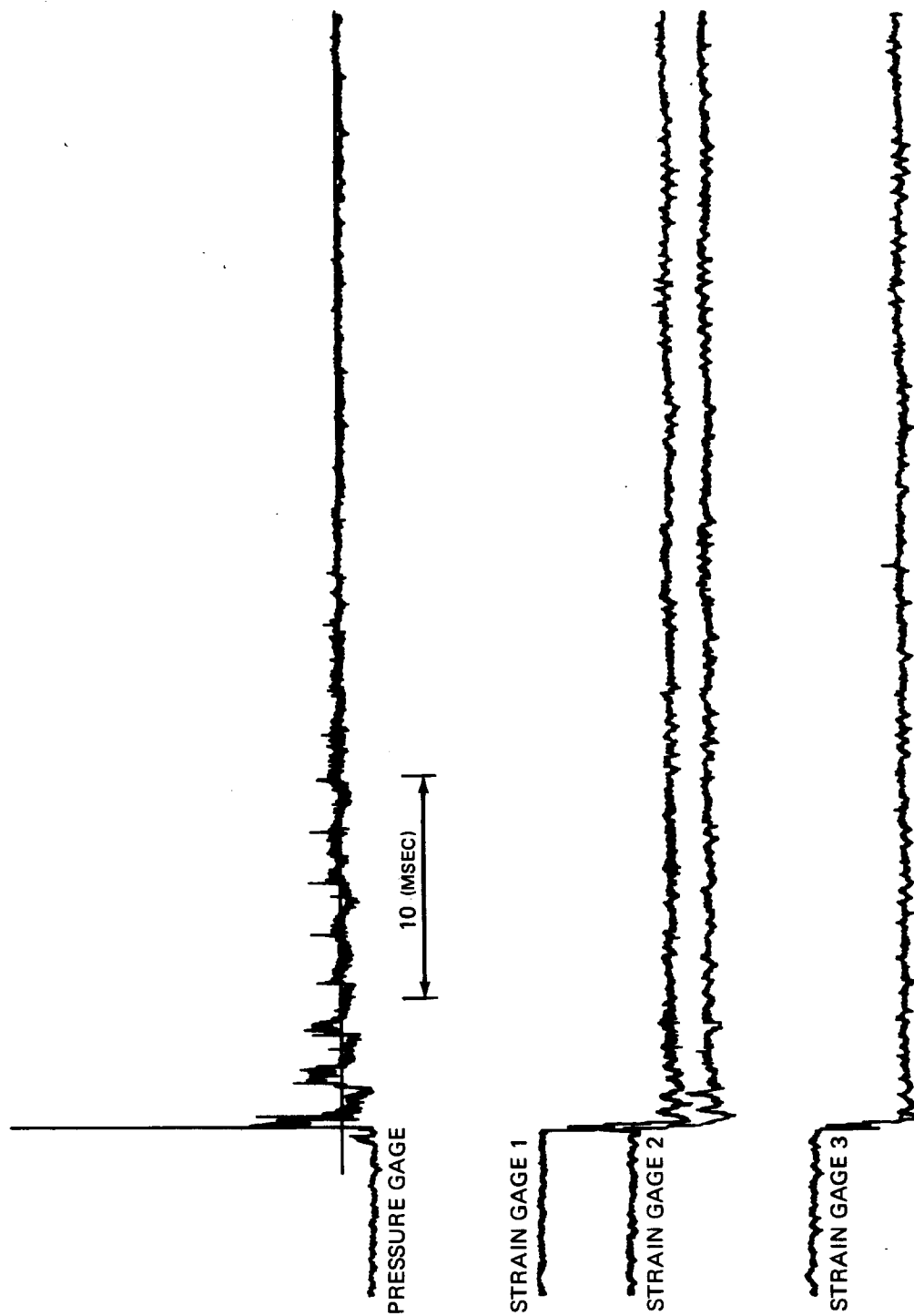
Figure 15d — Slow-Speed Playback of Test 100

36

1140 PSI

PRESSURE GAGE

1 (MSEC)

STRAIN GAGE 1

STRAIN GAGE 2

STRAIN GAGE 3

STRAIN GAGE 4

0.0393 IN/IN
0.0147 IN/IN
0.0312 IN/IN

GAGE 4 RADIALLY ALIGNED AT r = 5 IN.

FAILED
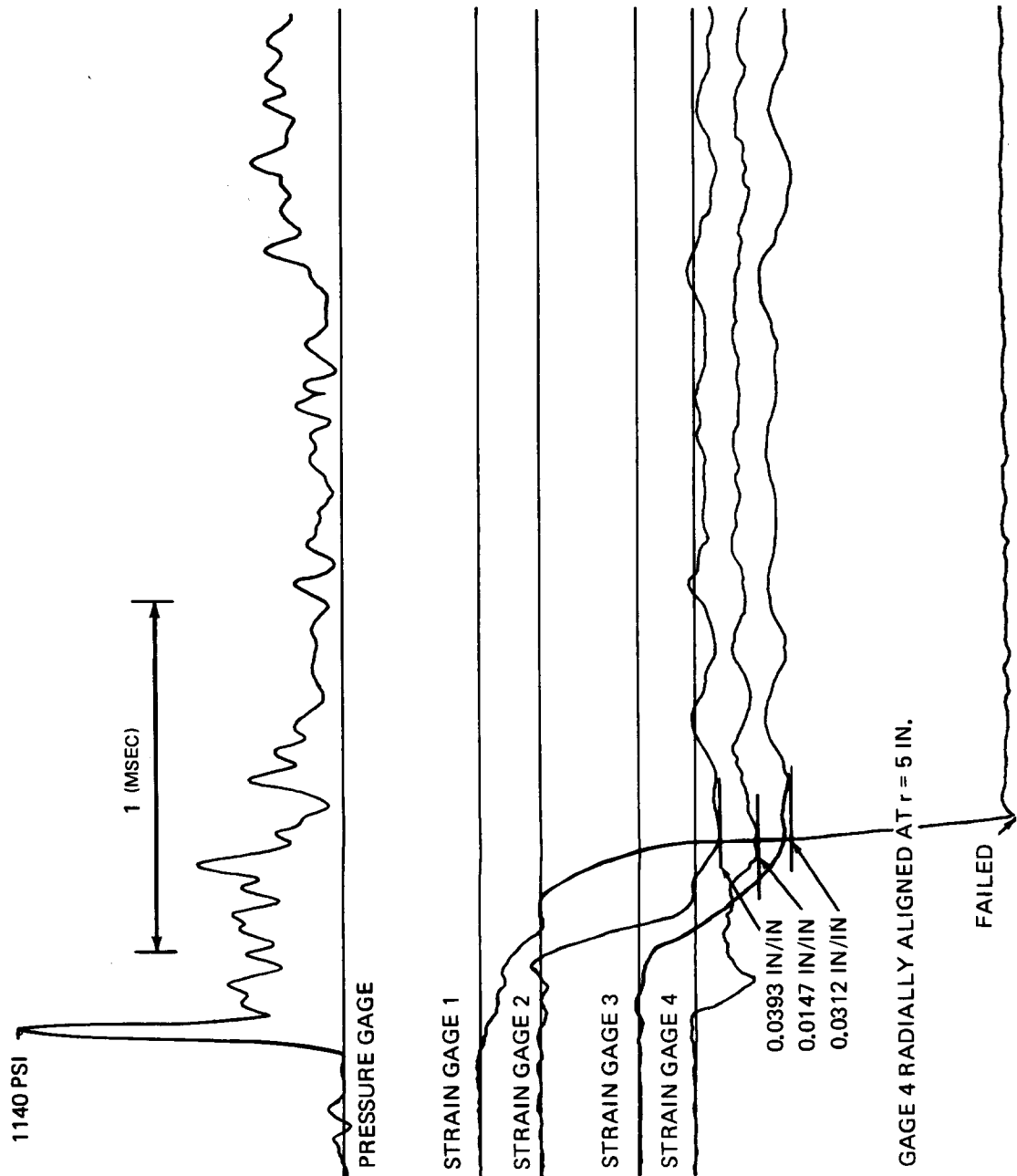
Figure 15e — High-Speed Playback of Test 107

(The 1/16-in. steel plate was loaded by a 15-g Pentolite charge detonated at the 35-in. SOD.
The resulting permanent deflection at the plate center was 1.15 in.)

37

10 (MSEC)

PRESSURE GAGE

STRAIN GAGE 1

STRAIN GAGE 2

STRAIN GAGE 3

STRAIN GAGE 4
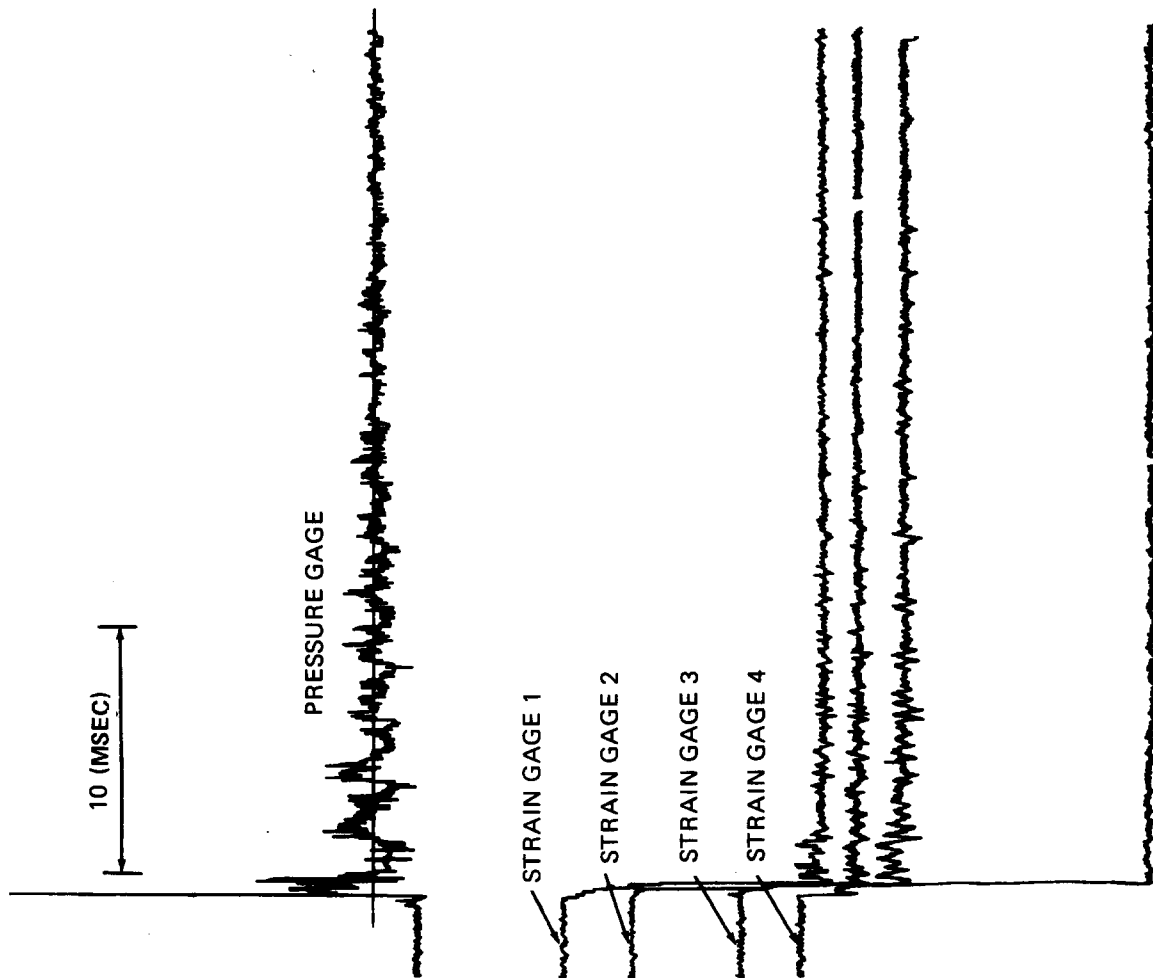
Figure 15f – Slow-Speed Playback of Test 107

38
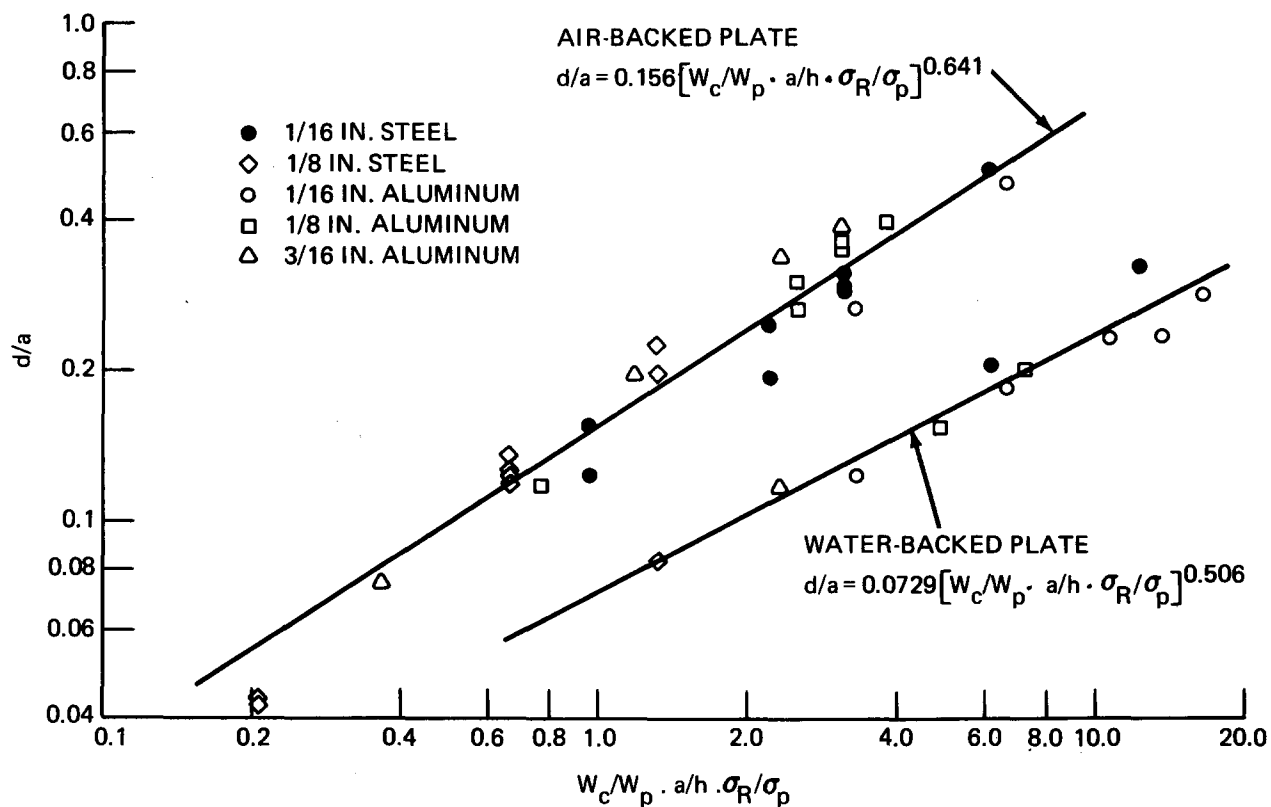
Figure 16a – Plates Tested on the Long Chamber
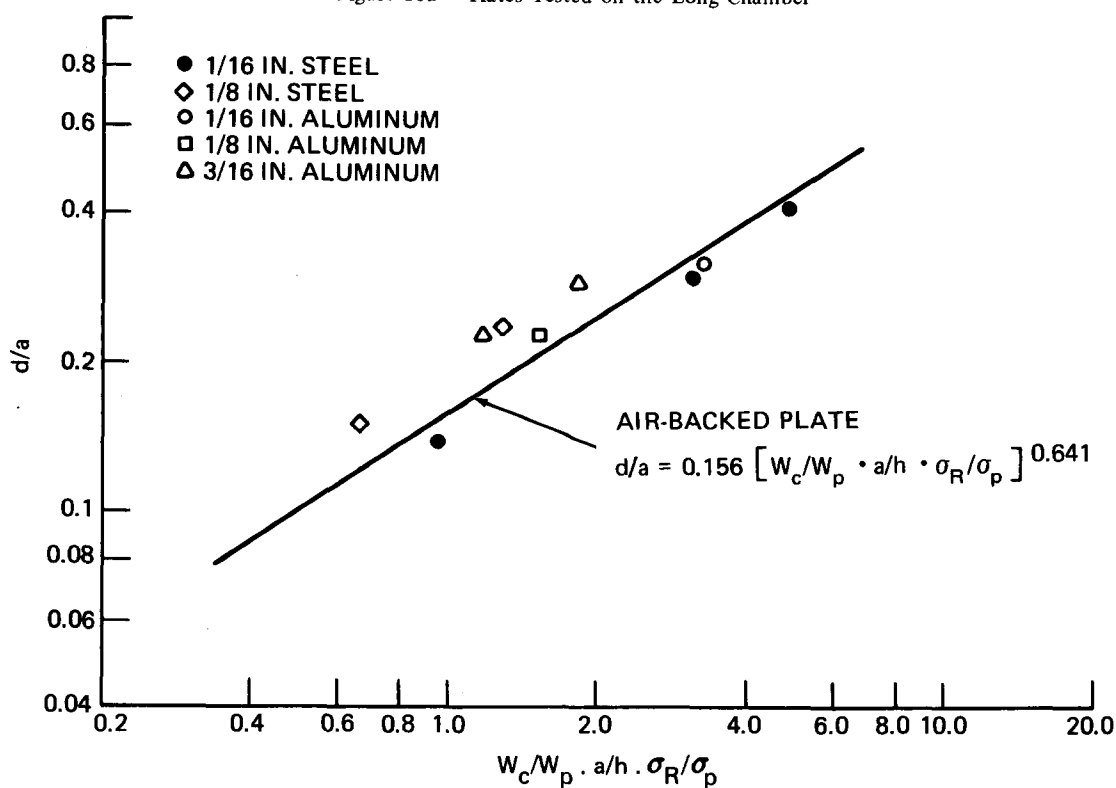
Figure 16b – Plates Tested on the Short Chamber

Figure 16 – Nondimensionalized Maximum Deflections of All Unfailed Plates

39

TEST 94 — 50G CHARGE VENTING THROUGH A 6.8-IN^2 HOLE

P_m

PRESSURE (PSI)

1400

VENTING ACCORDING TO PROCTOR 2

P_w

230

TIME (MSEC)

0   4   8   12   16   20   24   28   32   36
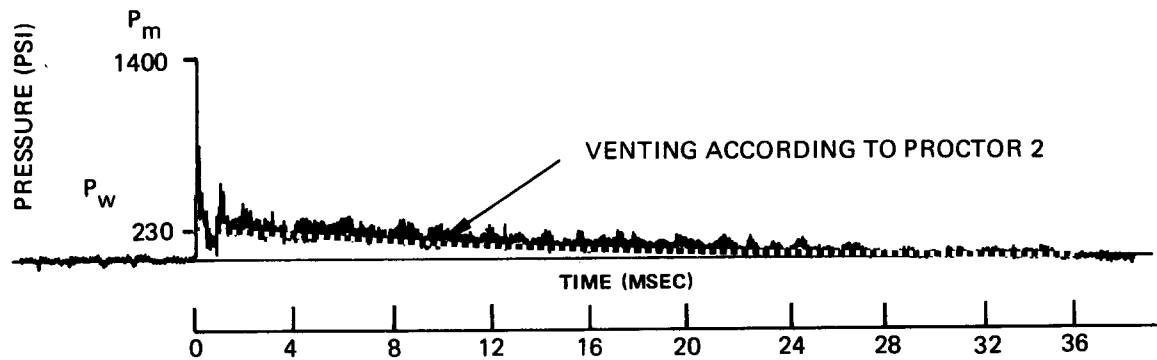
TEST 97 — 50G CHARGE VENTING THROUGH A 27.2-IN^2 HOLE

P_m

PRESSURE (PSI)

660

VENTING ACCORDING TO PROCTOR 2

P_w

230

TIME (MSEC)

0   4   8   12   16   20   24   28   32   36
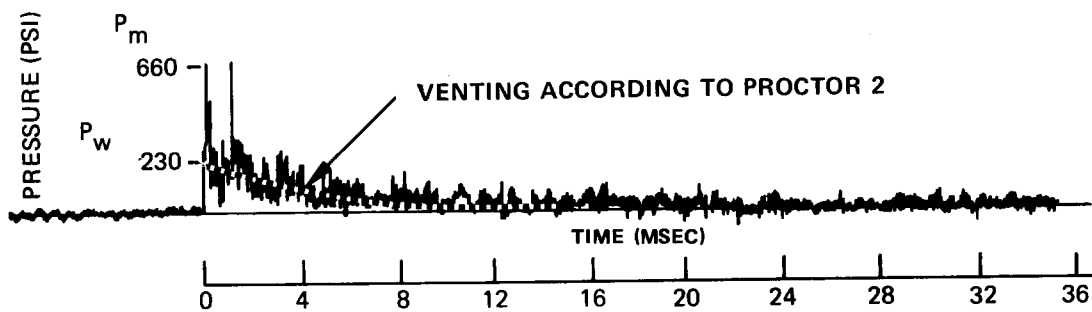
TEST 102 — 25G CHARGE VENTING THROUGH A 108-IN^2 HOLE

P_m

PRESSURE (PSI)

240

VENTING ACCORDING TO PROCTOR 2

142

P_w

TIME (MSEC)

0   4   8   12   16   20   24   28   32   36
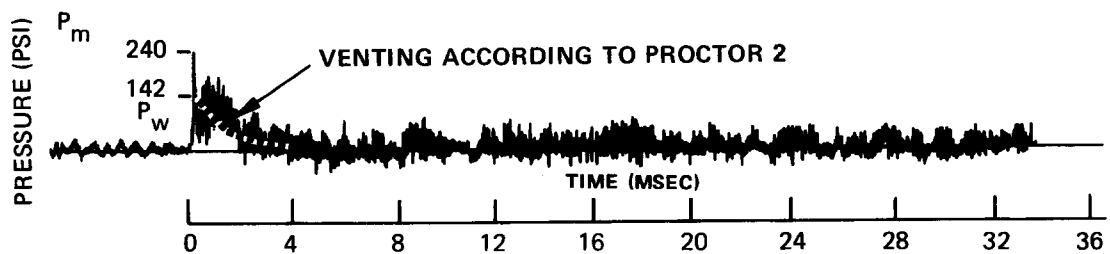
Figure 17 — Pressure Histories of Venting to the Atmosphere from a 2.26-Cubic Foot
Chamber through Different Venting Areas

40
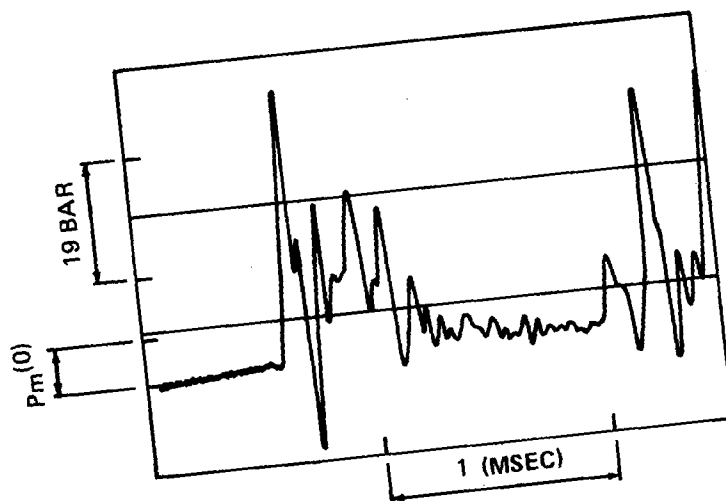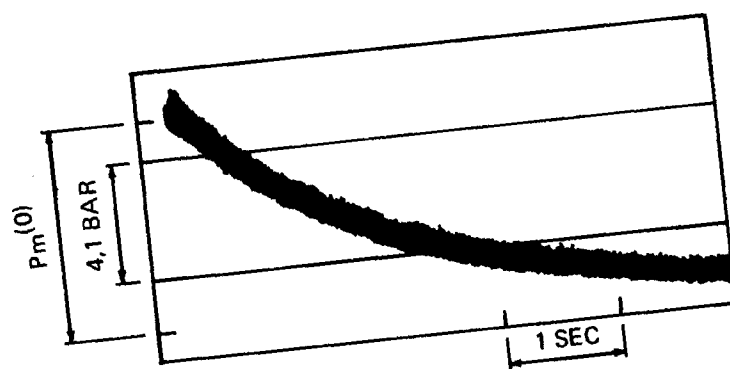
Figure 18 — Comparison between Predicted and Measured Maximum Pressure
(A and B represent the same event with different times scales; from Weibull[3])

TEST #17, 7gm CHARGE AT 35″ IN SOD
$P=1300\,e^{-13.7t}$; $t < 0.22$ MSEC
$P=61$ PSI; $t \geq 0.22$ MSEC

$P_m = 1300$

PRESSURE (PSI)

$P_w = 61$

0    $t_1=0.22$ 1   2

TIME (MSEC)

TEST #35, 25gm CHARGE AT 35″ IN SOD
$P=1700\,e^{-6.8t}$; $t < 0.37$ MSEC
$P=142$ PSI; $t \geq 0.37$ MSEC

$P_m = 1700$

PRESSURE (PSI)

$P_w = 142$

0    $t_1=0.37$ 1   2

TIME (MSEC)

TEST #55, 50gm CHARGE AT 35″ IN SOD
$P=1800\,e^{-3.9t}$; $t < 0.52$ MSEC
$P=230$ PSI; $t \geq 0.52$ MSEC

$P_m = 1800$

PRESSURE (PSI)

$P_w = 230$

0    $t_1=0.52$ 1   2

TIME (MSEC)
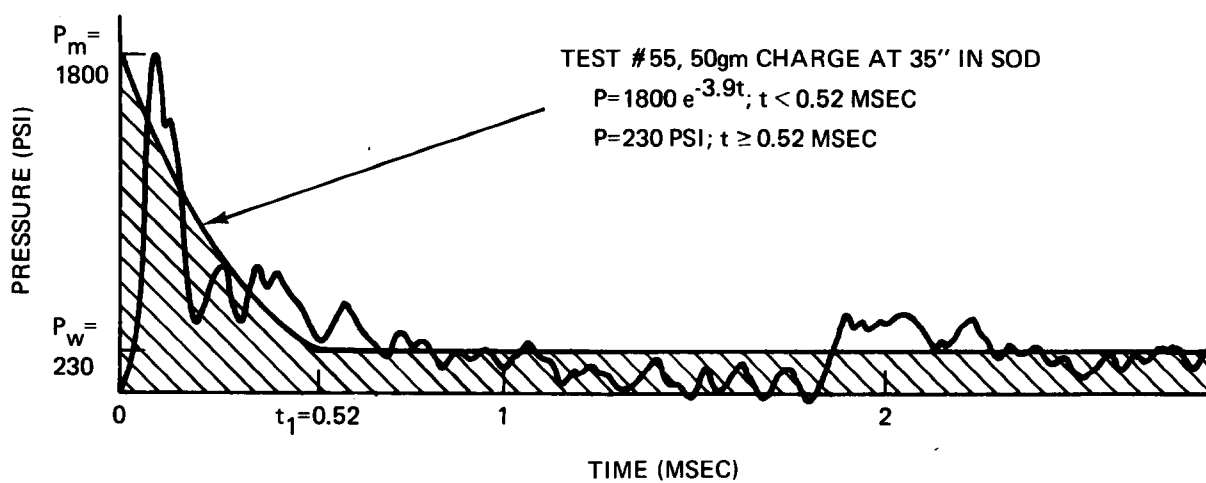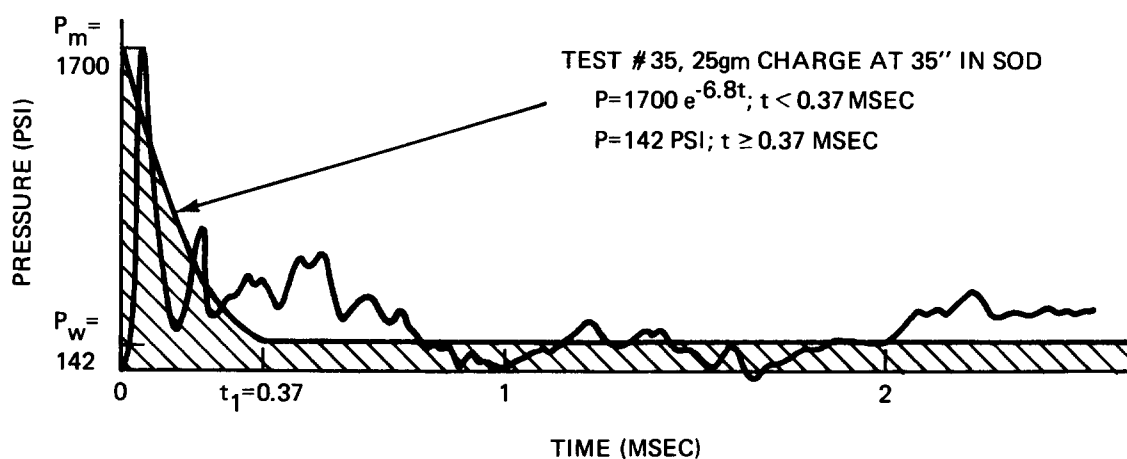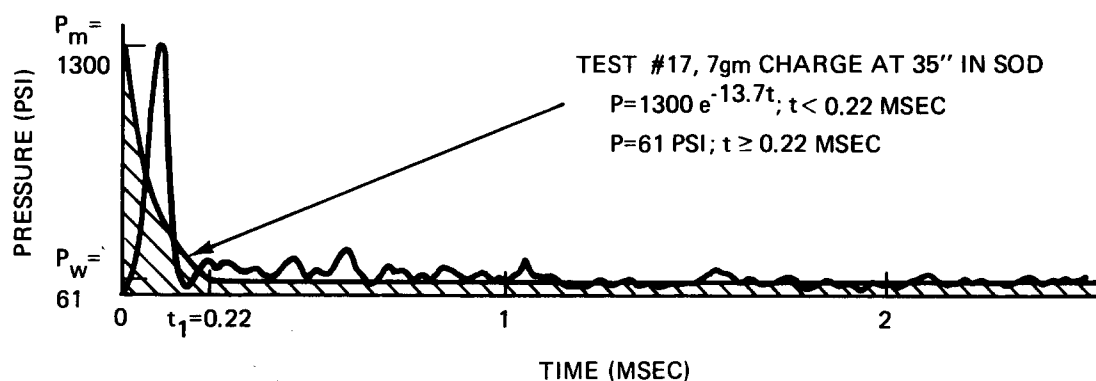
Figure 19 — Typical Measured and Synthesized Pressure Records

42

TABLE 1 – PEAK OVERPRESSURES RECORDED FOR AIR-BACKED PLATES

(Values are in pounds per square inch. Venting tests are not included.)

TABLE 1A – CHARGES DETONATED WHILE AT 35-INCH SOD MOUNTED AT THE PLUG

7-Gram Charge		15-Gram Charge		25-Gram Charge		50-Gram Charge		65-Gram Charge	
Test	Pressure	Test	Pressure	Test	Pressure	Test	Pressure	Test	Pressure
16	1000	20	1500	24	1100	52	2100	105	1370
17	1300	21	1200	25	1900	55	1800		
40	600	107	1140	27	2000	56	1500		
26	1500			34	1400	51^2	2400		
53	1700			35	1700				
47	850			49	3000				
98	865			50	1700				
18^4	900			54	1700				
23^3	700			84	1550				
19^2	700			103	1320				
22^2	800			87	2255				
38^2	800			99	2205				
39^2	400			100	2280				
				82	960				
				106	1530				
				48^2	1800				

TABLE 1B – CHARGES DETONATED AT SHORTER SOD

SOD in.	7-Gram Charge		25-Gram Charge	
	Test	Pressure	Test	Pressure
33			85	1350
31			83	530
25			89	2170
21	67	300	68	1000
	70	400	69	700
18			90	600
			77	635
			78	830
			79	1130
			80	1160
			81	545
12			101	940
			104	1220
6	71	1100	72	2500
	73	550	74	2300
			75	2000

Note: Unless otherwise indicated, all records were taken with the gage mounted in the flange as shown in Figure 5. Numerals after test numbers indicate that the gage was located face on in the rigid plate as follows:

    2 indicates mounted at r = 0 in.
    3 indicates mounted at r = 3 in.
    4 indicates mounted at r = 5 3/8 in.

More detailed information on individual test setups is given in Appendix B.

43

TABLE 2 — PLATE DEFLECTIONS

(An asterisk indicates that plate formed dimple at center; deflection was measured off-center at the side of the dimple)

TABLE 2A — PLATES MOUNTED ON 37-INCH CHAMBER

Air-Backed Plates				Water-Backed Plates			
Test No.	SOD in.	Charge Wt. g	Max. Defl. in.	Test No.	SOD in.	Charge Wt. g	Max. Defl. in.
(1/16-In. Medium Steel)							
1	35	7	0.92				
9		7	0.73				
107		15	1.15				
2		15	1.45				
3		25	1.78				
6		25	1.87				
106		25	1.76				
4		50	3.02	7	35	50	1.23
5	35	60	Failure	8	35	100	1.95
67	21	7	0.53				
68	21	25	1.22				
73	6	7	0.59				
74	6	25	1.29				
(1/8-In. Medium Steel)							
45	35	7	0.26				
98		7	0.25				
35		25	0.73				
49		25	0.75				
50		25	0.80				
100		25	0.72				
46		50	1.19				
56	35	50	1.33	66	35	50	0.50

1 of 3

Test No.		Charge Wt. (g)	Defl. (in.)
100	35	25	0.72
46	35	50	1.19
56	35	50	1.33
66	35	50	0.50
(1/16-In. Aluminum)			
26	35	7	1.58
28	35	15	2.84
27	35	25	Failure
57	35	7	0.73
58	35	15	1.11*
59	35	25	1.39*
61	35	32	1.43*
62	35	40	1.71*
60	35	50	Failure
75	6	25	Center failure
(1/8-In. Aluminum)			
29	35	7	0.70
30	35	25	1.61
24	35	25	1.80
31	35	32	2.18
36	35	32	2.15
37	35	40	2.40
44	35	50	Failure
63	35	50	0.93
64	35	75	1.21
(3/16-In. Aluminum)			
53	35	7	0.45
32	35	25	1.19
33	35	50	2.03
105	35	65	2.31
65	35	50	0.71

TABLE 2B – PLATES MOUNTED ON 18-INCH CHAMBER
(All plates were air backed and tested at 16-in. SOD)

Plate Type	Test No.	Charge Wt. g	Max. Defl. in.
1/16-In. Medium Steel	113	7	0.82
1/16-In. Medium Steel	114	25	1.76
1/16-In. Medium Steel	116	40	2.45

TABLE 2B – PLATES MOUNTED ON 18-INCH CHAMBER

(All plates were air backed and tested at 16-in. SOD)

Plate Type	Test No.	Charge Wt. g	Max. Defl. in.
1/16-In. Medium Steel	113	7	0.82
1/16-In. Medium Steel	114	25	1.76
1/16-In. Medium Steel	116	40	2.45
1/16-In. Medium Steel	115	50	Failure
1/8-In. Medium Steel	117	25	0.90
1/8-In. Medium Steel	118	50	1.41
1/16-In. Aluminum	119	7	1.87
1/16-In. Aluminum	120	15	Failure
1/8-In. Aluminum	122	15	1.37
1/8-In. Aluminum	121	25	Failure
3/16-In. Aluminum	123	25	1.36
3/16-In. Aluminum	124	40	1.71
3/16-In. Aluminum	125	57	Failure

TABLE 3 – CALCULATED AND MEASURED VENTING TIMES

Test No.	Vent Area ft^2	Charge Wt. gm	Chamber Volume ft^3	Calc. Peak Overpressure psi	Time to Critical Pressure	
					Calculated msec	Measured msec
102	0.754	25	2.26	142	2.0	3
95	0.188	7	2.26	61	6.3	8
96	0.188	25	2.26	142	7.8	9
97	0.188	50	2.26	230	8.3	12
109	0.047	7	1.13	100	14.9	15
93	0.047	7	2.26	61	25.1	35
91	0.047	25	2.26	142	31.8	29
94	0.047	50	2.26	230	33.1	38

TABLE 4 – CALCULATED AND MEASURED IMPULSES

(Values for calculated impulses are from NAVFAC[4])

Charge Size g	Standoff in.	Calculated Impulse psi-msec	Average Measured Impulse psi-msec	Range of Measured Impulses psi-msec	Range of Times (ti) msec	Number of Impulse Records for Case
	6	69	80	75, 85	0.19, 0.30	2
7	18–21	36	24	20, 28	0.20, 0.24	2
	35	90*	92	65–119	0.18–0.38	7
	6	160	148	142–153	0.19, 0.21	2
25	18–21	82	89	74–104	0.17–0.27	7
	35	230*	206	141–252	0.24–0.49	14
	6	268	––	––	––	0
50	18–21	134	––	––	––	0
	35	400*	372	342–402	0.47–0.59	3

Note: The integration was performed on all records obtained with the gage in the flange position for all tests except venting tests and tests where plate failure occurred. The integration was from t = 0 to t = t_1, where t_1 was as derived in this section as:

$$t_1 = -\frac{i \ln P_w/P_m}{P_m - P_w}$$

* A 2-in. standoff from the back wall was used to determine the impulse delivered to the back wall. This impulse was then assumed to reflect intact to the target plate; it was added to the direct impulse in order to arrive at the value given here.

APPENDIX A

INSTRUMENTATION

INTRODUCTION

In order to determine the pressure resulting from the detonation of the explosive charge and to measure the strain response of selected diaphrams, a recording system was installed in an instrumentation van located near the test area.

COMPONENTS OF THE RECORDING SYSTEM

1.   A bonded strain gage sensing element-type pressure transducer (Micro Systems Type PT 3S-C1) with its associated driver was used to measure pressures. Both static and dynamic calibrations were conducted to verify linearity and proper operation. The system gave linear readings over the entire 0- to 4000-psi static pressure range tested. The dynamic test was performed by mounting the gage onto a small water-filled chamber which was fitted with a piston at its top. A weight was dropped onto the piston, and the resulting pressure pulse in the chamber was measured by the gage. Since the drop height and mass of the weight were known, it was possible to calculate the theoretical peak pressure and time duration of the pressure pulse as described by Gesswein and Chertock.[5] They have shown that a sine pulse would result; use of their equations gave a value of 2820 psi for the peak pressure and one of 0.708 msec for the half-period of the sine pulse. As shown in Figure A.1 of this appendix, comparable experimental values were 2280 psi and 1.06 msec, respectively. Although the measured peak pressure was lower than the calculated value, the pressure record did show the correct total impulse; this can be seen in Figure A.1 by comparing the pressure record with the sine curve which contains the correct calculated total impulse.

Since the transducer would be exposed to temperatures exceeding its compensated range (30 to 130 F), a series of tests was conducted to determine the response of the transducer to rapid temperature changes; a photographic flashbulb was used as the heat source. The results of these tests indicated that the first 2 msec of a pressure record would not be appreciably affected by a rapid change in temperature.

---

[5]Gesswein, J. and G. Chertock, "A Dynamic Calibration Technique for Underwater Explosion Pressure Gages," David Taylor Model Basin Report 1328 (Sep 1959).

49

2.   Micro-Measurements Type EP-08-125AD-120 gages were used in most of the strain
gage tests. These gages are a high elongation, post-yield type and were installed with
Eastman 910 cement or AE-10 epoxy.

3.   A pressure transducer conditioner and amplifier (NSRDC Type 470-1A) was used to
supply power to the transducer driver, to provide balancing and shunt calibration networks,
and to amplify the transducer output signal.

4.   A strain gage conditioner and amplifier (NSRDC Type 450-2A) was used to supply
bridge voltage to the gage, to provide balancing and shunt calibration networks, and to
amplify the output from the strain gage.

5.   An FM tape recorder (Ampex CP-100) was used to record and reproduce the
amplified signals; a 5-kHz sine wave was also recorded for timing purposes.

6.   A string oscillograph (Consolidated Electrodynamics Corporation Type 5-124) with
Type 7-323 galvonometers was used for visual reproduction of the recorded signals.

        The components used are shown schematically in Figure A.2.

RECORDING TECHNIQUE

        The signals were recorded at a tape speed of 60 ips using FM electronics with a fre-
quency response of 0 to 20 kHz. Prior to each test, several calibration steps were recorded;
these were produced by shunting a known resistance across one arm of the bridge. A tape
speed of 1.875 ips was used for the playback of the signals onto the string oscillograph. At
this playback speed, the effective frequency response of the string galvonometers was 0 to
19 kHz.

SIGNAL GAIN AND DISTORTION CAUSED
TAPE RECORDER CHARACTERISTICS

        To test the ability of the recording system to record and reproduce signals rich in high
frequency components, square wave signals were fed into the recorder through the amplifier
and played back through the oscillograph. The playback records were characterized by rise
times of approximately 0.035 msec and short-duration "overshoots" of approximately
16 percent of the square wave amplitude (see Figure A.3). The rise times and overshoots
were constant throughout the 0- to 10-kHz frequency range tested and throughout a ten-
fold increase in amplitude. This rise time is long in comparison with the very short rise
times associated with the incident airblast shock waves. Thus considerable distortion in the
shape and magnitude of the initial pulse is to be expected.

The lowest frequency of the pressure gage plate sensing element is 140 kHz, corresponding to a maximum quarter period of 0.00176 msec or less. Thus the rise time of the tape recorder was at least 20 times the maximum possible quarter period of the gage, and the tape recorder limited the recorded signal rise time.

SIGNAL ATTENUATION CAUSED BY PRESSURE GAGE GEOMETRY

The ratio of average pressure $\bar{p}$ to maximum pressure p_m is obtained by averaging the pressure wave p as it sweeps across the circular face of the gage (Figure A.4).

$$\bar{p} = \frac{1}{A} \int_A \left[\frac{1}{T} \int_0^T p \, dt \right] dA$$

$$= \frac{1}{\pi a^2} \int_{-a}^{+a} \left[\frac{c}{2a} \int_0^{\frac{2a}{c}} p_M \, H\left(t - \frac{x}{c}\right) e^{-a\left(t - \frac{x}{c}\right)} dt \right] (2\sqrt{a^2 - x^2} \, dx)$$

$$\frac{\bar{p}}{p_M} = \frac{1}{\left(a \, \frac{a}{c}\right) \pi a^2} \int_{-a}^{+a} \left(1 - e^{-2a\frac{a}{c}} e^{a\frac{x}{c}}\right) \sqrt{a^2 - x^2} \, dx$$

$$= \frac{1}{2\beta} \left(1 - \frac{2e^{-2\beta}}{\pi} \int_{-1}^{+1} e^{\beta x} \sqrt{1 - x^2} \, dx\right), \, \beta \gtrsim 0.075$$

$$= \frac{1}{2\beta} \left[1 - e^{-2\beta} \left(1 + \frac{\beta^2}{8}\right)\right], \, \beta \lesssim 0.075$$

$$\text{where} \quad H\left(t - \frac{x}{c}\right) = \begin{cases} 0 & t < \frac{x}{c} \\ \frac{1}{2} & t = \frac{x}{c} \\ 1 & t > \frac{x}{c} \end{cases}$$

51

a is a positive decay constant,

$$\beta = a \; \frac{a}{c}$$

$$\chi = \frac{x}{a} \; , \text{ and}$$

$$e^{\beta \chi} = 1 + \beta\chi + \frac{\beta^2}{2} \; \chi^2 \quad \text{for } \beta \lesssim 0.075.$$

A plot of $\overline{p}/p_M$ is given in Figure A.5.

It should be noted that the above analysis is based on the assumption that the wave has a steep front and decays exponentially. This assumption has been observed to be valid for shock waves in tubes. It is also hypothesized that the gage is flush mounted rather than slightly recessed as for the tests reported herein. The diffraction phenomena associated with the recess have not been taken into account because of their complexity.

For the fairly representative value $a = 17.5(\text{msec})^{-1}$, Figure A.5 gives a ratio $\overline{p}/p_m = 88$ percent. The value of a was determined by measuring values of p_m, p_f, and t_f (as defined in Figure A.6) for typical pressure records by applying the relationship: $a = - \; [\text{Log}_e \; (p_f/p_m)]/t_f$ to find the corresponding value of a, and taking a mean of values so obtained.

The signal amplitude entering the electronics of the system is $\overline{p}$. As indicated earlier in discussing signal gain and distortion caused by tape recorder characteristics, the recorded pressure amplitude p_R is

$$p_R = 1.16 \; \overline{p}$$

But as noted in the preceding paragraph, $\overline{p}$ itself represents a reduction

$$\overline{p} = 0.88 \; p_m$$

Thus the overall relationship is

$$p_R = 1.16* \; 0.88* \; p_m = 0.98 \; p_m$$

It is not the intent of the authors to imply that this close correspondence of p_R and p_m is generally true. They wish only to convey the idea that the recorded pressure amplitudes ought at least to resemble the actual ones due to compensating errors in the recording process.

RECORDED
PRESSURE
PULSE

A SINE PULSE
CONTAINING
THE CORRECT
CALCULATED
IMPULSE

2,280 PSI

2000 PSI

1.0 MSEC T/2

1.06 MSEC
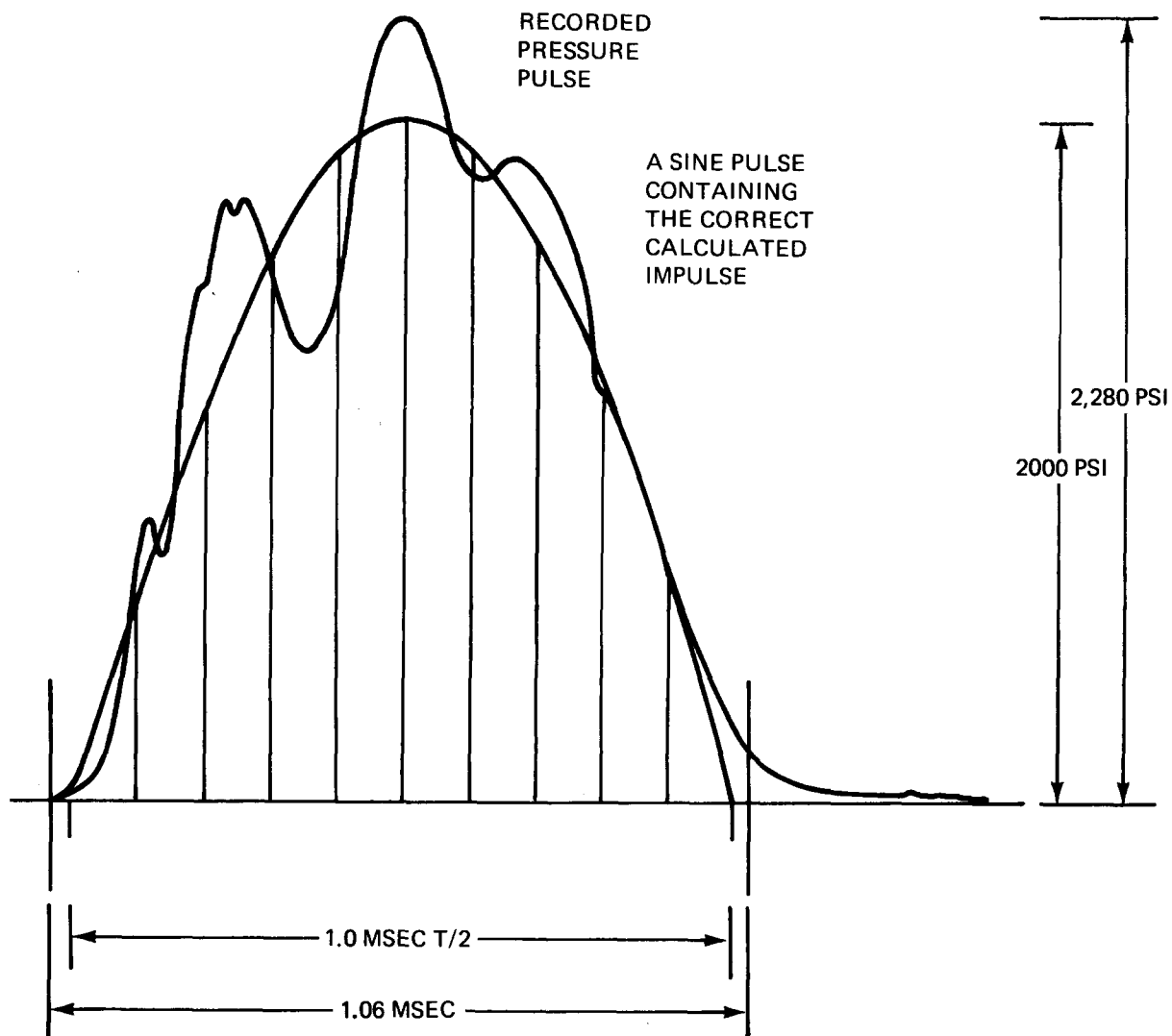
Figure A.1 — Dynamic Calibration of the Pressure Gage

PRESSURE
GAGE

CONDITIONER
AND AMPLIFIER
TYPE 470-1A

5 kHz

TAPE RECORDER
0 TO 20 kHz
AMPEX CP-100

STRING
OSCILLOGRAPH
0-19 kHz

STRAIN
GAGE

CONDITIONER
AND AMPLIFIER
TYPE 450-2A
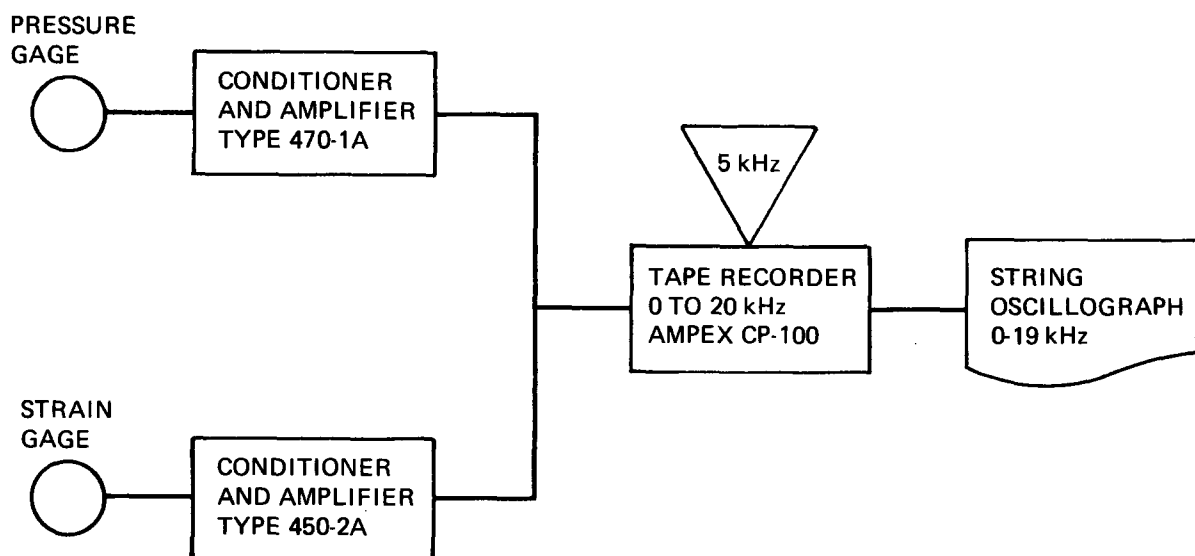
Figure A.2 — Instrumentation Components
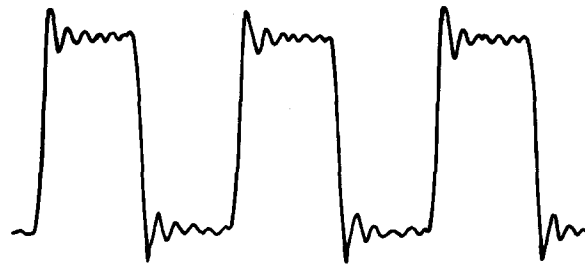
Figure A.3 — A 2-KC Square Wave as Recorded by the Amplifier-Tape
Recorder Segment of the Recording System
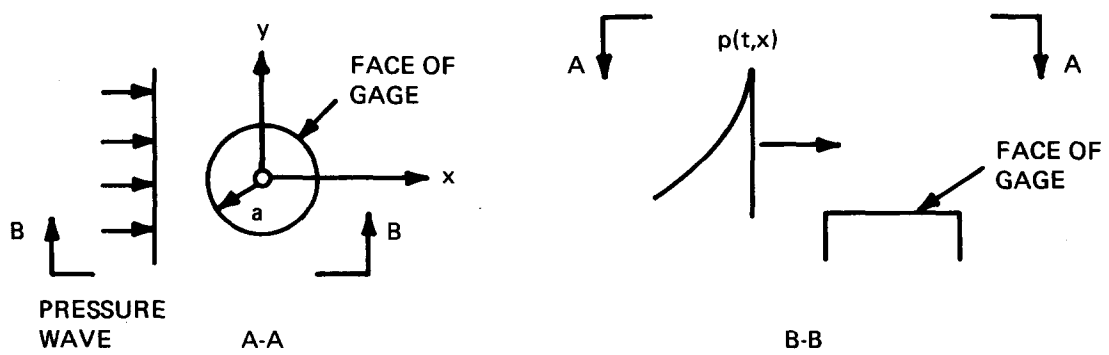

Figure A.4 — Passage of Wave over Gage
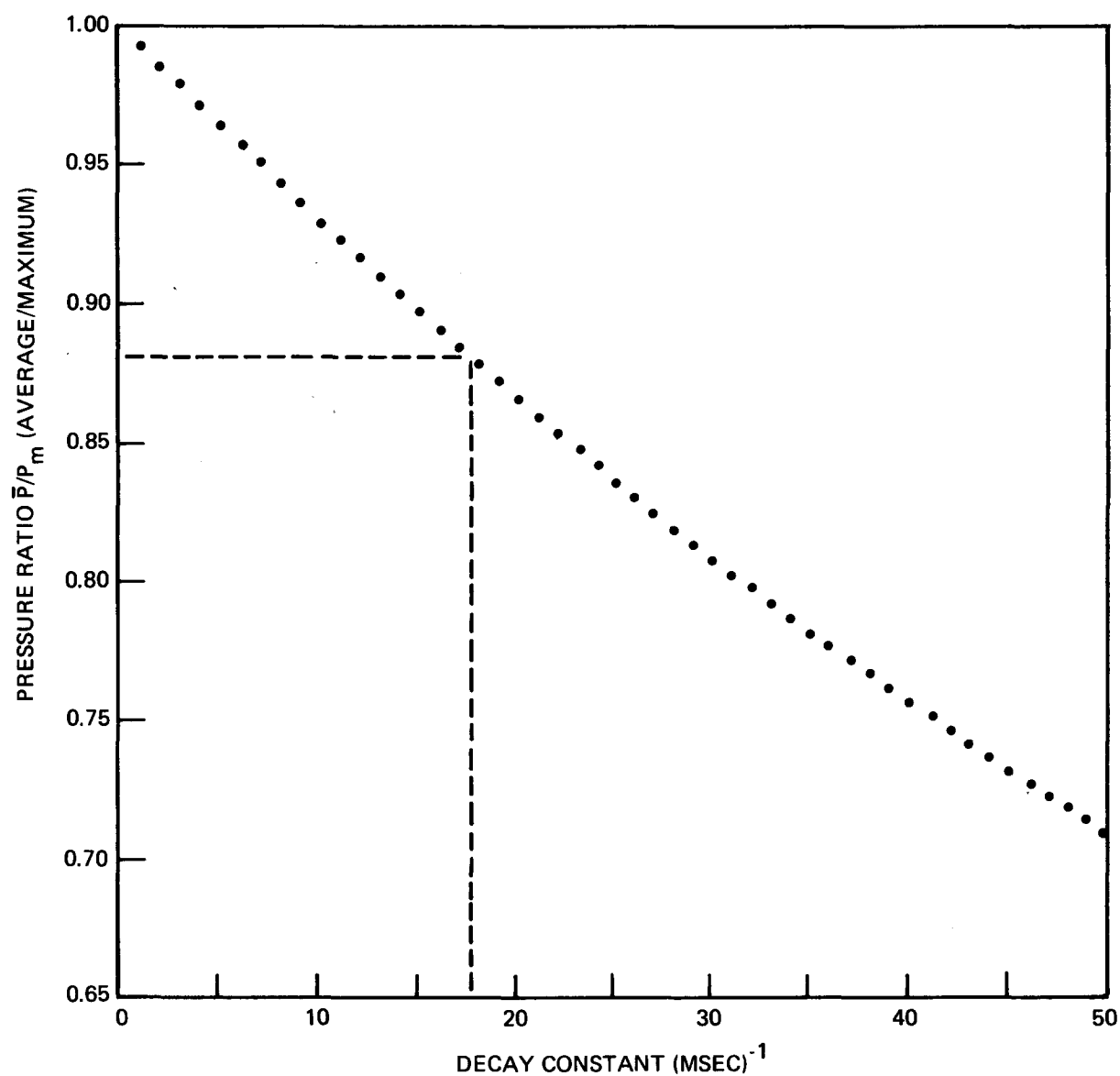
Figure A.5 — Ratio of Average Pressure to Maximum Pressure versus Decay Constant
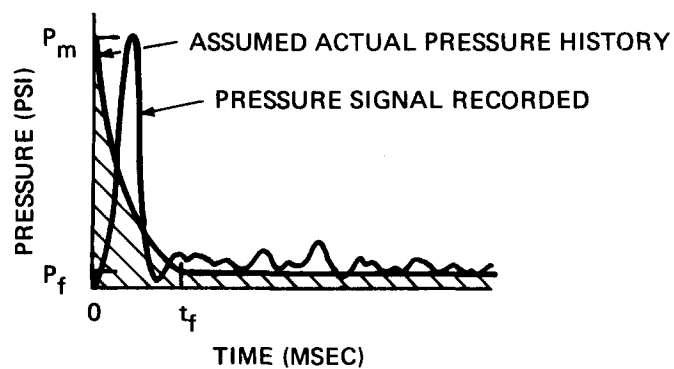
Figure A.6 — Determination of Decay Constant a

APPENDIX B
SUMMARY OF TEST DATA

In Table B.1, water-backed plate tests are indicated by a W after the plate type; all other tests were air backed. Permanent deflections were measured at the plate center except for water-backed plates which formed dimples. Those deflections were measured at the side of the dimple where the deflection was greatest; deflections so measured are indicated by a D following that deflection value in the table. Superscript numbers following peak pressure values indicate pressure gage location:

1. Mounted in the flange and side on to the charge
2. Mounted at $r = 0$ in the rigid plate, face on to the charge
3. Mounted at $r = 3$ in. in the rigid plate, face on to the charge
4. Mounted at $r = 5\ 3/8$ in. in the rigid plate, face on to the charge

Amplifying remarks for test numbers marked by an asterisk in Table B.1 are as follows:

Test	9	Five strain gages mounted; most failed during test
Test	47	Plate lined with 1/2 in. thick, high-density styrofoam
Test	49	Three strain gages mounted; two gages failed
Test	50	Three strain gages mounted; all failed
Tests	54–56	Plate lined with 1/2 in. thick, high-density styrofoam
Test	88	System not grounded; electrical noise destroyed signal
Test	98	Three strain gages mounted; none failed
Test	99	Same plate as Test 98; gage failed; deflection listed is cumulative deflection after Tests 98 and 99.
Test	100	Three strain gages mounted; none failed
Tests	106,107	Four strain gages mounted; center gage failed in both tests
Test	108	Pressure gage rendered inoperable during test; bad record obtained
Tests	110,111	Noise in signal and zero point shift gave unusable pressure records
Test	112	Severe zero point shift rendered gage inoperable

TABLE B.1 – LISTING OF ALL TESTS

(Excluding calibrations (Tests 10–15 and 41–43) and missfires (Tests 76, 86, and 92).)

TABLE B.1a – TESTS PERFORMED WITH THE 37-INCH CHAMBER

Test No.	Information Sought	Charge Weight g	Charge Range in.	Plate Type	Permanent Deflection in.	Peak Pressure psi
1	Response	7	35	1/16 In. Steel	0.92	—
2		15			1.45	—
3		25			1.78	—
4		50			3.02	—
5		65			Failure	—
6		25		1/16 In. Steel	1.87	—
7		50		1/16 In. Steel – W	1.23	—
8		100		1/16 In. Steel – W	1.95	—
9*	Response	7		1/16 In. Steel	0.73	—
16	Loading	7		Rigid	—	1000[1]
17		7		Rigid	—	1300[1]
18		7			—	900[4]
19		7			—	700[2]
20		15			—	1500[1]
21	Loading	15	35	Rigid	—	1200[1]

58

Test No.	Information Sought	Charge Weight g	Charge Range in.	Plate Type	Permanent Deflection in.	Peak Pressure psi
22	Loading	7	35	Rigid	—	800[2]
23	Loading →	7		Rigid →	—	700[3]
24	Loading	25			—	1100[1]
25	Loading	25		Rigid	—	1900[1]
26	Response/ Loading	7		1/16 In. Aluminum	1.58	1500[1]
27	Response/ Loading	25		1/8 In. Aluminum	Failure	2000[1]
28	Response	15		1/16 In. Aluminum	2.84	—
29		7		1/8 In. Aluminum	0.70	—
30		25		1/8 In. Aluminum	1.61	—
31		32		1/8 In. Aluminum	2.18	—
32		25		3/16 In. Aluminum	1.19	—
33	Response	50		3/16 In. Aluminum	2.03	—
34	Response/ Loading	25		1/8 In. Aluminum	1.80	1400[1]
35	Response/ Loading	25	35	1/8 In. Steel	0.73	1700[1]
36	Response	32		1/8 In. Aluminum	2.15	—
37	Response	40		1/8 In. Aluminum	2.40	—

59

Test No.	Information Sought	Charge Weight g	Charge Range in.	Plate Type	Permanent Deflection in.	Peak Pressure psi
38	Loading	7	35	Rigid	—	800²
39	Loading	7		Rigid	—	400²
40	Loading	7		Rigid	—	600¹
44	Response	50		1/8 In. Aluminum	Failure	—
45	Response	7		1/8 In. Steel	0.26	—
46	Response	50		1/8 In. Steel	1.19	—
47*	Loading	7		Rigid	—	850¹
48	Loading	25		Rigid	—	1800²
49	Response/ Loading	25		1/8 In. Steel	0.75	3000¹
50*	Response/ Loading	25		1/8 In. Steel	0.80	1700¹
51	Loading	50		Rigid	—	2400²
52	Loading	50		Rigid	—	2100¹
53	Response/ Loading	7		3/16 In. Aluminum	0.45	1700¹
54*	Loading	25		Rigid	—	1700¹
55*	Loading	50	35	Rigid	—	1800¹

Test No.	Information Sought	Charge Weight g	Charge Range in.	Plate Type	Permanent Deflection in.	Peak Pressure psi
56*	Response/Loading	7	35	1/8 In. Steel	1.33	1500[1]
57	Response	7		1/16 In. Alum. – W	0.73	—
58		15		1/8 In. Alum. – W	1.11 D	—
59		25		1/16 In. Alum. – W	1.39 D	—
60		50			Failure	—
61		32			1.43 D	—
62		40		1/16 In. Alum. – W	1.71 D	—
63		50		1/8 In. Alum. – W	0.93	—
64		75		1/8 In. Alum. – W	1.21	—
65		50	35	3/16 In. Alum. – W	0.71	—
66	Response	50	35	1/8 In. Steel – W	0.50	—
67	Response/Loading	7	21	1/16 In. Steel	0.53	300[1]
68	Response/Loading	25	21	1/16 In. Steel	1.22	1000[1]
69	Loading	25	21	Rigid	—	700[1]
70	Loading	7	21	Rigid	—	400[1]

61

Test No.	Information Sought	Charge Weight g	Charge Range in.	Plate Type	Permanent Deflection in.	Peak Pressure psi
71	Loading	7	6	Rigid	--	1100[1]
72	Loading	25	6	Rigid	--	2500[1]
73	Response/Loading	7	6	1/16 In. Steel	0.59	550[1]
74	Response/Loading	25	6	1/16 In. Steel	1.29	2300[1]
75	Response/Loading	25	6	1/16 In. Aluminum	Failure	2000[1]
77	Loading	25	18	Rigid	--	635[1]
78		25	18		--	830[1]
79		25	18		--	1130[1]
80		25	18		--	1160[1]
81		25	18		--	545[1]
82		25	35		--	960[1]
83		25	31		--	530[1]
84		25	35		--	1550[1]
85		25	33		--	1350[1]
87		25	35		--	2255[1]
88	Loading	25	25	Rigid	--	--

Test No.	Information Sought	Charge Weight g	Charge Range in.	Plate Type	Permanent Deflection in.	Peak Pressure psi
89	Loading	25	25	Rigid	—	2170[1]
90	Response/Loading	25	18	1/16 In. Aluminum	Failure	600[1]
91	Venting	25	18	6.8 In.² Hole	—	740[1]
93		7	18	6.8 In.² Hole	—	415[1]
94		50	18	6.8 In.² Hole	—	1400[1]
95		7	18	27.2 In.² Hole	—	195[1]
96		25	18	27.2 In.² Hole	—	710[1]
97	Venting	50	18	27.2 In.² Hole	—	660[1]
98*	Response/Loading	7	35	1/8 In. Steel	0.25	865[1]
99*	Response/Loading	25	35	1/8 In. Steel	0.66	2205[1]
100*	Response/Loading	25	35	1/8 In. Steel	0.72	2280[1]
101	Response/Loading	25	12	1/16 In. Aluminum	Failure	940[1]
102	Venting	25	18	No Plate	—	240[1]
103	Loading	25	35	Rigid	—	1320[1]
104	Response/Loading	25	12	1/16 In. Aluminum	Failure	1220[1]
105		65	35	3/16 In. Aluminum	2.31	1370[1]
106*		25	35	1/16 In. Steel	1.76	1530[1]
107*		15	35	1/16 In. Steel	1.15	1140[1]
108*	Response/Loading	25	9	1/16 In. Aluminum	Failure	—

TABLE B1.b – TESTS PERFORMED WITH THE 18-INCH CHAMBER

Test No.	Information Sought	Charge Weight g	Charge Range in.	Plate Type	Permanent Deflection in.	Peak Pressure psi
109	Venting	7	9	6.8 In.² Hole	—	305[1]
110*		25	9	6.8 In.² Hole	—	—
111*		50	9	6.8 In.² Hole	—	—
112	Venting	50	9	6.8 In.² Hole	—	—
113	Response	7	16	1/16 In. Steel*	0.82	—
114		25	16	1/16 In. Steel	1.76	—
115		50	16	1/16 In. Steel	Failure	—
116		40	16	1/16 In. Steel	2.45	—
117		25	16	1/8 In. Steel	0.90	—
118		50	16	1/8 In. Steel	1.41	—
119		7	16	1/16 In. Aluminum	1.87	—
120		15	16	1/16 In. Aluminum	Failure	—
121		25	16	1/8 In. Aluminum	Failure	—
122		15	16	1/8 In. Aluminum	1.37	—
-123		25	16	3/16 In. Aluminum	1.36	—
124		40	16	3/16 In. Aluminum	1.71	—
125	Response	57	16	3/16 In. Aluminum	Failure	—

64

TABLE B.2 – MATERIAL PROPERTIES OF SPECIMEN PLATES FROM TENSILE TESTS

Plate Type	Average Thickness	Stress at 0.2 Percent Offset Yield Point	Stress at Ultimate Yield Point	Elongation (in 2 inches) at Breaking Load	Original Cross-Sectional Area	Reduction in Area at Breaking Load	Breaking Load (Approximate)
in.	in.	ksi	ksi	percent	in.	percent	lb
1/16 In. Medium Steel	0.055	36.9	49.7	73	0.027	66	600
1/8 In. Medium Steel	0.112	45.4	57.5	60	0.056	67	2500
1/16 In. Aluminum	0.064	24.4	32.2	23	0.032	70	750
1/8 In. Aluminum	0.128	25.5	34.4	26	0.063	54	1800
3/16 In. Aluminum	0.188	24.8	32.9	27	0.093	59	2300

65

CENTER DEFLECTION AND FAILURE AS A FUNCTION OF CRITICAL IMPULSE DELIVERED IN A CRITICAL TIME

The critical time t_c is one-fourth of the natural period. The natural period is calculated as (see page 450 in Timoshenko[6])

$$p = \frac{\alpha}{a^2} \sqrt{\frac{gD}{\gamma h}}$$

where $D = Eh^3/12\,(1-\nu^2)$,

    h is thickness in inches,

    $\gamma h/g$ is the mass per unit area of plate (slugs per inch^2),

    a is plate radius in inches, and

    $\alpha = 10.21$.

The critical impulse is calculated from $I_c = \rho\,\delta\,V_c$ as in Sewell and Kinney.[1] Here V_c is taken as 200 ft/sec for steel and 240 ft/sec for aluminum. The minimum Heaviside pressure to failure is I_c/t_c.

Values for t_c are given in Table C.1 for each plate type. This table also gives ratios of minimum pressures. The minimum mean pressure achieved in the chamber was taken as simply the Weibull[3] pressure. Comparisons with pressure records showed that the Weibull pressure was a lower bound to the actual mean pressure at early time. The ratio of this Weibull pressure to the calculated minimum mean pressure to failure is listed in Table C.2 as a check on the failure criterion, one which is independent of the pressure records. As can be seen, plates survived at actual mean pressures well above the minimum mean pressures calculated by the method of Sewell and Kinney.[1]

TABLE C.1 – CRITICAL IMPULSE AND CRITICAL TIMES OF THE
TEST PLATES

Plate Type	Critical Time t_c msec	Critical Impulse I_c psi-msec	Minimum Mean Pressure to Failure psi
1/16 In. Steel	1.6	96.5	60
1/8 In. Steel	0.82	197	240
1/16 In. Aluminum	1.4	46.4	33
1/8 In. Aluminum	0.72	93.0	129
3/16 In. Aluminum	0.49	136	278

[6]Timoshenko, S., "Vibration Problems in Engineering," Third Edition, D. Van Nostrand Company, Inc., Princeton, New Jersey (Jan 1955).

TABLE C.2 – COMPARISON OF CALCULATED AND MEASURED CRITICAL IMPULSES

(The measured impulses for all tests at the 35-in. SOD were interpolated from the average impulse curves of Figure 11 of this report. Impulses at closer SOD were read from individual impulse curves. In all cases the impulse was read at the critical time t_c).

Plate Type	Test No.	Charge Range in.	Ratio of Minimum Mean Pressure Achieved to Calculated Minimum Mean Pressure Required for Failure	Ratio of Impulse Measured in Time t_c to Calculated Critical Impulse for Failure	Deflection at Plate Center in.
1/16-Inch Steel	1	35	1.37	2.20	0.92
	9		1.37	2.20	0.73
	2		2.25	3.46	1.45
	107		2.25	3.46	1.15
	3		3.20	4.18	1.78
	6		3.20	4.18	1.87
	106		3.20	4.18	1.76
	4		5.20	5.66	3.02
	5	35	6.28	7.34	Failure
	67	21	1.37	0.84	0.53
	68	21	3.20	3.77	1.22
	73	6	1.37	1.73	0.59
	74	6	3.20	3.14	1.29
1/8-Inch Steel	45	35	0.30	0.79	0.26
	98		0.30	0.79	0.25
	35		0.80	1.65	0.73
	49		0.80	1.65	0.75
	50		0.80	1.65	0.80
	100		0.80	1.65	0.72
	46		1.30	2.34	1.19
	56		1.30	2.34	1.33
1/16-Inch Aluminum	26	35	2.48	4.32	1.58
	28		3.94	6.90	2.84
	27	35	5.82	8.41	Failure
	75	6	5.82	4.32	
	101	12	5.82	5.74	
	104		5.82	6.90	
	90	18	5.82	4.74	Failure
1/8-Inch Aluminum	29	35	0.64	1.56	0.70
	30		1.49	3.33	1.61
	34		1.49	3.33	1.80
	31		1.70	3.66	2.18
	36		1.70	3.66	2.15
	37		2.07	4.19	2.40
	44		2.42	4.62	Failure
3/16-Inch Aluminum	53	35	0.30	0.85	0.45
	32		0.69	1.84	1.19
	33		1.12	2.65	2.03
	105	35	1.35	2.98	2.31

DOCUMENT CONTROL DATA - R & D

(Security classification of title, body of abstract and indexing annotation must be entered when the overall report is classified)

1. ORIGINATING ACTIVITY (Corporate author)	2a. REPORT SECURITY CLASSIFICATION
Naval Ship Research and Development Center Bethesda, Maryland 20034	**UNCLASSIFIED**
	2b. GROUP

3. REPORT TITLE

THE RESPONSE OF CLAMPED CIRCULAR PLATES TO CONFINED EXPLOSIVE LOADINGS

4. DESCRIPTIVE NOTES (Type of report and inclusive dates)

Final Report

5. AUTHOR(S) (First name, middle initial, last name)

Steve Zilliacus, Wayne E. Phyillaier and Paul K. Shorrow

6. REPORT DATE	7a. TOTAL NO. OF PAGES	7b. NO. OF REFS
February 1974	72	6

8a. CONTRACT OR GRANT NO.	9a. ORIGINATOR'S REPORT NUMBER(S)
b. PROJECT NO. In-House Independent Research Program Task Area ZR011-01-01	3987
c. Report Preparation Task Area SF 43.422.701.04 d. NSRDC Work Unit 1749-400	9b. OTHER REPORT NO(S) (Any other numbers that may be assigned this report)

10. DISTRIBUTION STATEMENT

Approved for public release: distribution unlimited.

11. SUPPLEMENTARY NOTES	12. SPONSORING MILITARY ACTIVITY
	Naval Ship R & D Center Bethesda, Maryland 20034

13. ABSTRACT

A series of confined explosive tests was carried out for 12-in.-diameter steel and aluminum plates. Each plate in turn formed one end of the closed cylindrical chamber inside which the explosives were detonated. Tests were conducted with the chamber suspended in air and in water to determine pressure histories, deformation shapes, and failure modes in the inelastic range of air- and water-backed plates as well as to determine pressure decay rates resulting from venting to the atmosphere.

The final deformation shapes observed were uniform and repeatable, but the pressure records were less uniform. There was a distinct difference between the final shapes of the air- and water-backed plates; those of the former were intermediate between conical and parabolic whereas those of the latter were more parabolic and sometimes dimpled in the center. Failures occurred at the plate edge for charge standoffs greater than one plate diameter and at the plate center for closer standoffs. Measured pressure decays due to venting confirmed an analytical method established for predicting gas venting.

14. KEY WORDS	LINK A		LINK B		LINK C	
	ROLE	WT	ROLE	WT	ROLE	WT
Response of Circular Plates to Explosive Loading						
Explosive Deformation of Circular Plates						
Plate Response to Confined Explosions						
Blast Deformation of Circular Plates						